Formula Student Front Wing Design According to Aerodynamics Principle

Sarawin Arunnitithum

Titiwut Sinpo

A THESIS SUBMITTED IN PARTAL FUFILLMENT

OF THE REQUIREMENT FOR THE DEGREE OF

BACHELOR OF ENGINEERING IN MECHANICAL ENGINEERING

FACULTY OF ENGINEERING

KING MONGKUT'S INSTITUTE OF TECHNOLOGY LADKRABANG

2022

THESIS PROJECT OF YEAR 2022

MECHANICAL ENGINEERING FACULTY OF ENGINEER

KING MONGKUT'S INSTITUTE OF TECHNOLOGY LADKRABANG

Project Title Formula Student Front Wing Design According to Aerodynamics Principle

Student Name

1. Sarawin Arunnitithum Student ID 62011241
2. Titiwut Sinpo Student ID 62011283

_____ Advisor

(Asst.Prof. Chinda Charoenphonphanich)

Formula Student Front Wing Design According to Aerodynamics Principle

Sarawin Arunnitithum Student ID 62011241
Titiwut Sinpo Student ID 62011283
Asst.Prof. Chinda Charoenphonphanich Advisor

Academic year 2022

Abstract

Formula student is a racing competition. It was created to bring out student's potential in the field of automotive. The car must be built to the best performance and safety. The competition first held in Thailand in the year of 2006 by TSAE (Thailand Society of Automotive Engineers). KMITL (King Mongkut's Institute Technology of Ladkrabang) is also one of the teams that attends to the competition by building a car with high performance engine and efficient body under the specifications and rules of the competition. This thesis focuses on the front wing which is one of the parts that makes the car's body efficient according to aerodynamics by designing an airfoil and putting it at best angle to generate huge amount of downforce with the least drag and create great air flow around the car. The process started by choosing an airfoil that gives the best performance by using CFD simulation along with comparing the result to the standard one. After the airfoil is chosen, the 3-element front wing is drawn in 3D to use for the simulation of finding the angles of all 3 elements that give the best lift and drag coefficient. The simulation is done by Fluent in Ansys program using K-omega SST model. The result we get after trials of setting angle of attack is 5,13,25 which it gives 1.212 of lift coefficient and 1.992 of drag coefficient.

ACKNOWLEDGEMENT

This thesis is completed due to the advice, expertise, and experience from Assistant Professor Dr. Chinda Charoenphonphanich who is the advisor of this project. As same as other professors and our friends, they all deserve the acknowledgement, without them, this thesis would not be successful.

Finally, we would like to thank King Mongkut's Institute of Technology Ladkrabang that provides us such a great curriculum and also the support and resources to make this project completed.

Sarawin Arunnitithum

Titiwut Sinpo

TABLE OF CONTENT

LIST OF TABLES

LIST OF FIGURES

Chapter 1
INTRODUCTION

1.1 STATEMENT AND SIGNIFICANCE OF THE PROBLEMS

Formula student competition is organized by SAE (Society of Automotive Engineers) for university students to form teams to build their best car and compete with others. All parts and systems in the car are craft and build to gain as much performance as it could. The most important system in all kinds of vehicle is engine, but no matter how good the engine's performance is, without a nice body design that could guide the car through massive air flow while running at high speed, it could diminish the engine's performance and could lead to an accident that would severely injure the driver. For the car to thrust through the air, it needs to be able to control the air. The only component that could do that is the front wing because it's the first part of the vehicle that hits the air and the flow of the air in and out of front wing will affect the whole car. So, this thesis is made to help develop the front wing for KMITL Formula team according to the laws of Aerodynamics.

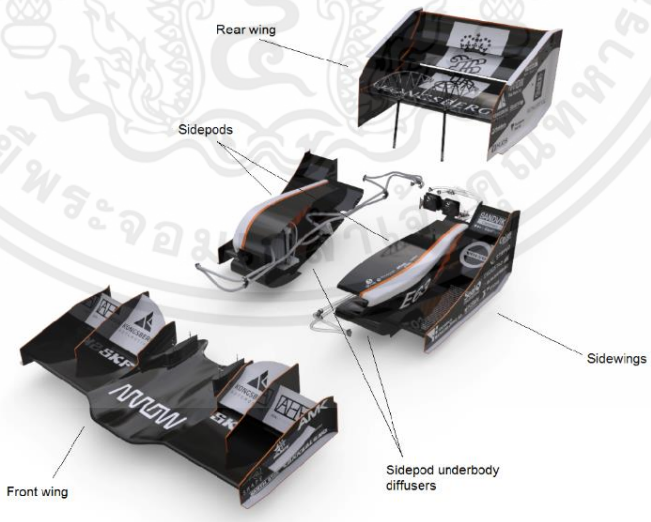

Figure 1.1 Formula student front wing

(https://www.semanticscholar.org)

1.2 GOAL AND OBJECTIVE

1.2.1 Study Aerodynamics theory and principle

1.2.2 Learn to use Ansys for simulation

1.2.3 Apply the knowledge of Aerodynamics to use for front wing adjustment

1.3 HYPOTHESIS TO BE TESTED

1.3.1 Better air flow around the car will make the car goes faster without any improvement to the engine.

1.4 SCOPE OR LIMITATION OF THE STUDY

1.4.1 The front wing development must meet with the rules of the competition.

1.4.2 The thesis validation will be done by comparing the result with the reference research and there will be no testing in the wind tunnel.

1.4.3 There will be no testing on the real car after the thesis is done.

1.5 PROCESS OF THE STUDY

1.5.1 Study related theory and literature

1.5.2 Learn to use Ansys for simulation

1.5.3 Review the rules of the competition about front wing designing

1.5.4 Simulate the latest version front wing of KMITL formula student team to see the result of the air flow.

1.5.5 Select 5 types of airfoils and simulate at various angle of attack

1.5.6 Collect all data to calculate to find which create the best air flow

1.5.7 Compare the result with reference research to validate

CHAPTER 2
LITERATURE REVIEW

2.1 Introduction

This document will discuss the design decisions and rational behind the Front Wing for NFR16. The Front Wing is positioned below the nosecone and front bulkhead, and consists of six individual wing elements (three on each side of the assembly) and one center splitter, all attached using four endplates. These individual components are made of various carbon fiber sandwich structures. The Front Wing is intended to provide downforce around the front region of the car, increasing the amount of available traction the vehicle has under the three dynamic states of acceleration, cornering, and braking.

2.1.1 Goals

- System must comply with all of Article 9 from the FSAE 2016 Rules
- Establish a first-year aerodynamic baseline for aerodynamic devices for the team
- Develop a manufacturing method that can be easily reproduced for the future
- Produce a maximum of 350lbs of downforce in conjunction with the rear wing system at a speed of 60 mph
- Allow some form of adjustability for purposes of balance and drivability

2.2 Design Overview

Item	Value
Frontal Area	1.12 m^2
C_L	-1.84
C_D	0.98

Figure 2.1 Overall performance
(https://static1.squarespace.com)

2.2.1 Airfoil Shape

To establish a first-year aerodynamic baseline for the front wings, airfoil shape was selected at the beginning of the design process. Shape was chosen based on a balance of performance with manufacturability. Three alternatives were considered, based on literature review of papers published by other FSAE teams: the Selig S1223, the Eppler E423, and the LNV109A. Using XFLOW, theoretical angle of attack vs coefficient of lift curves were generated for the three airfoil shapes, as shown in Figure 1. Using this information, the Eppler E423 was selected, as it has similar performance to the Selig S1223 while maintaining gentler stall characteristics and significantly simpler manufacturability of the trailing edge.

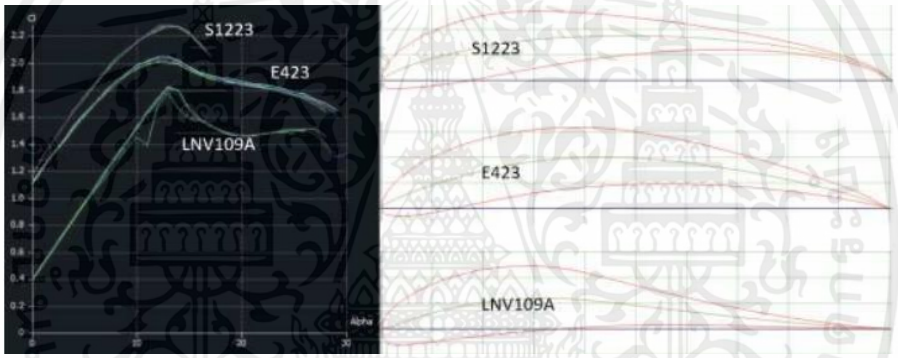

Figure 2.2 Performance comparison of three airfoil shapes. Angle of attack is plotted on the x-axis, and coefficient of lift is plotted on the y-axis.

(https://static1.squarespace.com)

2.2.2 Chord Length & Number of Elements

The front wing system was analyzed with the potential to be either a 2-element or 3-element wing system. Consulting the Competitive Car Aerodynamics book suggested that a 3-element system would be superior to a 2-element system, as doing so helps delay flow separation to allow higher angles of attack, which are necessary given the small working area as defined by regulations. A 2-element system was also analyzed using Star-CCM+, and in doing so was further determined to be inferior to a 3-element system. The optimal 2-element design, consisting of one 14” chord length element and one 5” chord length element at 5° and 43° relative to the ground plane, respectively,

only produced 86 lbs of downforce with 39 lbs of drag – a CL/CD ratio of 2.2. All higher angle-of-attack designs using the 2- element system was additionally plagued with flow separation. A screenshot of this design is shown below in Figure 2. Switching to a 3-element system eliminated the flow separation issue at similar angles of attack, allowing increased angles of attack and thus increased downforce. In order to fit three wing elements within the required height restrictions (maximum 9.8" above ground, further limited by suspension travel), chord lengths for the three elements were frozen at 8", 4", and 4".

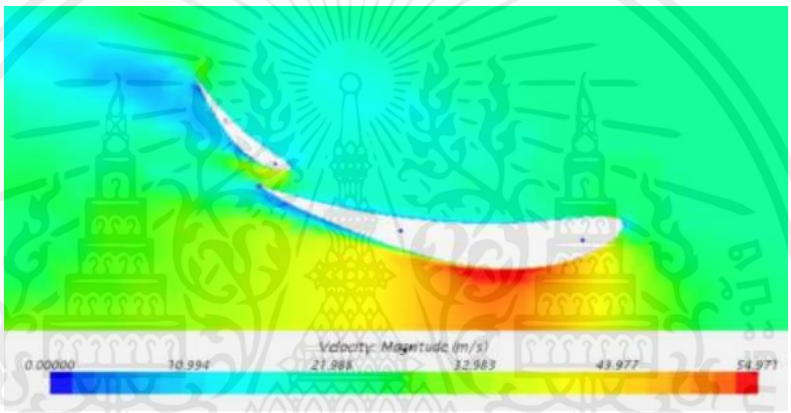

Figure 2.3 The most effective 2-element front wing design found. The large element has a chord length of 14" and is at 5° relative to ground, while the small element has a chord length of 5" and is at 43° relative to ground. Note the flow separation especially prevalent behind the smaller element.

(https://static1.squarespace.com)

2.2.3 Element Positioning

Computational fluid dynamics (CFD) using StarCCM+ was utilized to determine angles of attack and gap sizes for the front wing elements. CFD setup used the K-Ω Turbulence model, a 3mm base mesh size, and 8 prism layers to improve accuracy close to the boundary layer. Ultimately, four separate angle-of-attack arrangements were developed in conjunction with the rear wing. The angles of attack shown below are in order from front element, middle element, and back element. These settings provide a Front/Rear balance of 60/40, 50/50, 40/60, and 33/67, respectively.

- Front-heavy setting: -3°, 18°, 48°
- Even-balance setting: -3°, 18°, 26°
- Rear-heavy setting: -3°, 18°, 16°
- Acceleration setting: -3°, 0°, 3°

The first stage of front wing analysis was done with a simplified model of the front of the car, as shown in Figure 3 below. Final design stages were done with a (simplified) full car model, including the rear wing.

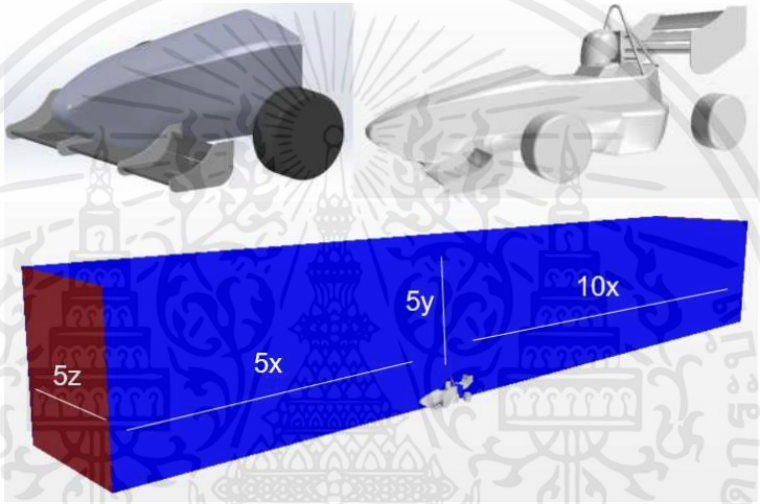

Figure 2.4 The front-car model used for preliminary front wing analysis on the left, and the simplified full-car model used for final aerodynamic system design on the right. On the bottom, the fluid volume used for all simulations is shown.
(https://static1.squarespace.com)

The front element was selected to be oriented at a negative angle relative to ground to allow for higher angles of attack for the second two elements. With the front element parallel to the ground (0°), the maximum downforce attained using CFD was 109 lbs at 60 mph. With the front element at an angle of attack of -3° relative to the ground, the maximum downforce attained was -116 lbs at 60 mph. Next, -3° was compared with -5°. For this stage in the analysis, the maximum downforce attained from a wing system using the front element at -3° was -27 lbs at 30 mph, while the maximum downforce attained from a wing system with front element at -5° was smaller, at -23 lbs

at 30 mph. Note that these systems used much higher angle of attacks than were actually feasible by regulations (these designs did not take suspension travel into account when limiting system height to 9.8” above the ground). Even so, the front element was frozen to be at -3° relative to ground for the remainder of the design cycle.

Next, the maximum allowable angle of attack, given height restrictions, for the 3rd element was estimated. This estimation was done assuming the 2nd element would be at roughly half the angle of attack as the 3rd element, the total gap size summed across all elements would be 0.5 inches in height, and 1 inch of clearance is required for the front wing under full car jounce conditions. As shown below in Table 1, this method yielded a maximum 3rd wing angle of attack of 48°. So, the maximum angle of attack for the 3rd element was frozen to be 48° relative to ground.

Table 2.1 Estimating the maximum allowable height for the 3rd element of the front wing, based on height restrictions.

3rd Element AoA [°]	Height Remaining [in]
70	-1.38
68	-1.27
66	-1.16
64	-1.04
62	-0.92
60	-0.79
58	-0.66
56	-0.52
54	-0.38
52	-0.23
50	-0.08
48	0.08
46	0.23
44	0.40
42	0.57
40	0.74
38	0.91
36	1.09
34	1.27
32	1.45
30	1.64

With the 1st and 3rd element angle of attacks frozen, CFD in Star-CCM+ was used to identify the ideal angle of attack for the 2nd element. From this point on, analysis was performed using the simplified full car model, as opposed to the simplified front-of-car model. As shown in Table 2 below, this positioning was identified to be 18°. So, the 2nd element was frozen to be at 18° relative to the ground.

Table 2.2 CFD results for the 2nd element of the front wing.

AoA [°]	C_L	L/D
20	-2.02	-6.13
18	-2.08	-6.23
15	-1.75	-6.40
12	-1.57	-7.27

The final stage of angle-of-attack design was developing multiple positions to allow for balance adjustability. The maximum angle-of-attack design yields a front/rear tire force balance of 60/40. To simplify adjustability in the physical system, only the 3rd element was selected to be adjustable for this purpose. So, keeping all other angles of attack constant, the angle of attack of the 3rd element was systematically decreased and balance calculated to determine potential settings for a 50/50 and 40/60 setting. In addition, one setting for the system with very low angles of attack was selected to serve as a low-drag, low-downforce setting for the acceleration event. This setting was selected arbitrarily to be -3° (keeping the main element un-adjustable), 0°, and 3° for the 1st, 2nd, and 3rd elements, respectively. Final angles of attack for all adjustable positions for the front wing system are shown in Table 3 below.

Table 2.3 Final adjustable settings to allow balance adjustability for the entire vehicle. Balance is Front/Rear, centered on the corresponding tires.

Front Wing (aoa)	Rear Wing (aoa)	Balance
-3,18,48	6,29,52	60/40
-3,18,26	6,29,52	50/50
-3,18,16	6,29,52	40/60
-3,0,3	6,16,26	accel

2.2.4 Endplate Design

Endplate shape was designed based on qualitative results from water tunnel testing and literature, which recommend larger endplates as opposed to close-to-element shape, and especially aesthetics. A video of the water tunnel test can be seen here: https://www.youtube.com/watch?v=FeYSxXnyT3s. The use of CFD was omitted from this year's design stage to allow a focus on wing element angle of attack. The final front endplate design, in CAD, is shown in Figure 4. The same endplate design was used for all four endplates, for manufacturing simplicity. The entire system, in CAD, is shown in Figure 5

Figure 2.5 Final front endplate design, in CAD.
(https://static1.squarespace.com)

Figure 2.6 Final front wing system, in CAD. Shown is the maximum angle of attack setting: -3°, 18°, 48°.

(https://static1.squarespace.com)

Chapter 3

THEORY

3.1 Front wing

Front wing is the most crucial part in all kinds of vehicle, consider in the aspect of Aerodynamics. It is the first part the air hit while moving toward it. The flow of the air throughout the vehicle depends on how the air leaves front wing so shape, size, and degree of attack are essential when designing the element.

3.1.1 Role of Front wing

By dividing the air that hits front wing, it generates downforce with high pressure that pushes the wing down to keep the car stick to the ground as it goes through curve with high speed. Although, the more downforce it generates, the more drag occurs to the car. So, the role of front wing is to generates the most downforce with the least drag.

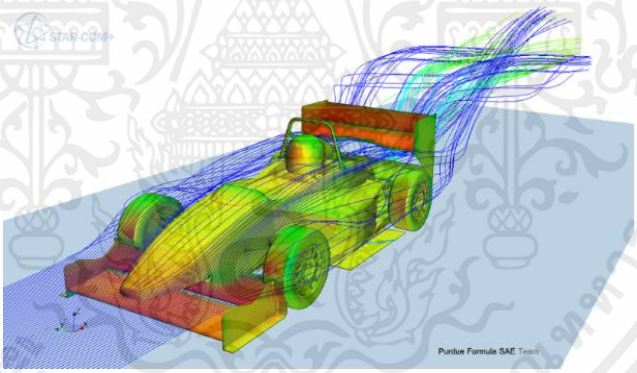

Figure 3.1 Front wing's role
(https://engineering.purdue.edu)

3.1.2 Material

With all the roles of the front wing and as it is a shield to the car, a strong material is needed to make this element. Steel is known as one of the strongest materials but it comes with lots of weight and that is not what any race car want. Material which is commonly use to craft race car parts is carbon fiber because of its strength and small amount of weight.

3.2 Aerodynamics

Literally, Aerodynamics consists of the word “Aero” and “Dynamics”. Aero simply means air. Dynamics is the study that deal with force and motion or something that is moving. Combine both meaning then Aerodynamics is the study of the force of air acting on moving object. The force can be distinguished into 4 kinds by the direction each is heading, which are lift, weight, thrust, and drag.

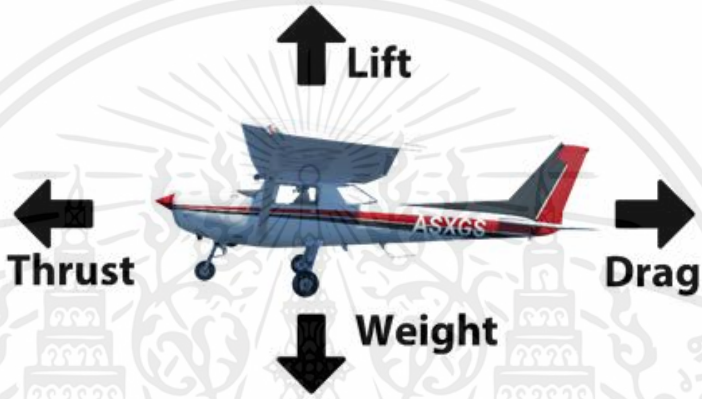

Figure 3.2 Aerodynamics forces
(https://forums.flightsimulator.com)

- Weight is the force going in the same direction of gravity or simply the weight of the object.
- Lift is the force acting to the opposite direction of weight or acting against it.
- Drag is the force that goes against the moving object and will slow it down.
- Thrust is the opposite of drag, it goes in the same direction with the object, so the force is helping the object to go faster.

All kinds of force can be useful depends on application. For example, an aircraft needs huge amount of lift and thrust force to fly in the air and accelerate forward, or a Formula 1 car that needs huge amount of downforce to stick to the ground while speeding 300-400 km/hr. This thesis uses Aerodynamics theory for Formula car development so the forces that relate and need to be considered in this topic are downforce and drag.

3.2.1 Drag

Drag is a force of fluid acting against any moving object which in this case is the air that surround a moving car. Drag occurs by 2 factors of the moving object: its shape and its surface. These 2 factors make 2 types of drag force. First, friction drag (skin drag) is shear stress acting on the surface of the object.

The equation of friction drag can be written as:

$$D_f = \frac{1}{2} C_d \rho \vartheta^2 A$$

Table 3.1 Empirical equation for the flat plate drag coefficient

Equation	Flow Conditions
$C_{Df} = 1.328/(\mathrm{Re}_\ell)^{0.5}$	Laminar flow
$C_{Df} = 0.455/(\log \mathrm{Re}_\ell)^{2.58} - 1700/\mathrm{Re}_\ell$	Transitional with $\mathrm{Re}_{x,cr} = 5 \times 10^5$
$C_{Df} = 0.455/(\log \mathrm{Re}_\ell)^{2.58}$	Turbulent, smooth plate
$C_{Df} = [1.89 - 1.62 \log(\varepsilon/\ell)]^{-2.5}$	Completely turbulent

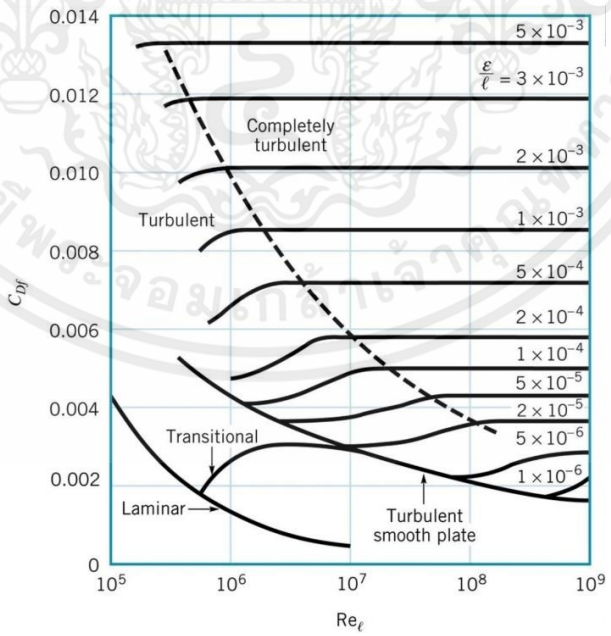

Figure 3.3 Friction drag coefficient for a flat plate parallel to the upstream flow (https://www.chegg.com)

The table 3.1 and Figure 3.3 shows how drag vary on flat plate with the effect of different flow conditions.

Second, pressure drag (shape drag) formed by force acting to the shape and size of the object.

The equation of pressure drag can be written as:

$$D_p = \int p \cos\theta \, dA$$

Pressure Drag Coefficient is expressed as:

$$C_{Dp} = \frac{D_p}{\frac{1}{2}\rho\vartheta^2 A}$$

The overall drag coefficient is calculated by the equation below:

$$C_D = C_{Df} + C_{Dp}$$

D_f is the friction drag

D_p is the pressure drag

C_d is the drag coefficient

ρ is the mass density of the fluid

ϑ is the velocity of the object

A is the cross-sectional area

The figure below shows that the blunter the body, the more drag coefficient is created.

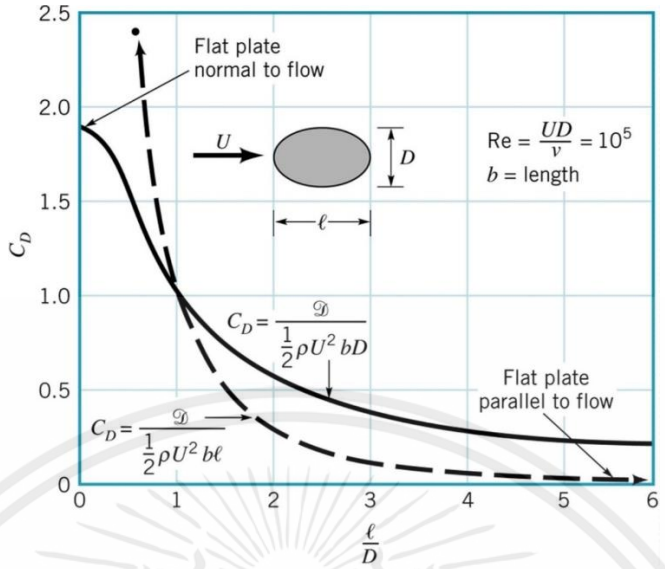

Figure 3.4 Drag coefficient for an ellipse with the characteristic area either the frontal area, $A = bD$, or the platform area, $A = bl$

(https://www.chegg.com)

Reynolds number is also another compiler that affects drag coefficient. It is divided into 3 ranges:

1. Low Reynolds number $(Re < 1)$
2. Moderate Reynolds number $(10^3 < Re < 10^5)$
3. Large Reynold number

For low Re, drag can be calculated from the equation:

$$D = C\mu lU$$

Where C is constant

Combine the equation of low Reynolds number drag with the equation of drag coefficient:

$$C_D = \frac{D}{\frac{1}{2}\rho U^2 l^2} = \frac{2C\mu lU}{\rho U^2 l^2} = \frac{2C}{Re}$$

The equation of low Reynolds number is shown below:

$$Re = \frac{\rho U l}{\mu}$$

Low Reynolds Number Drag Coefficients (Ref. 7) ($Re = \rho UD/\mu$, $A = \pi D^2/4$)

Object	$C_D = \mathcal{D}/(\rho U^2 A/2)$ (for $Re \lesssim 1$)	Object	C_D
a. Circular disk normal to flow	20.4/Re	c. Sphere	24.0/Re
b. Circular disk parallel to flow	13.6/Re	d. Hemisphere	22.2/Re

Figure 3.5 Low Reynold number drag coefficient (https://www.chegg.com)

As the Reynold number increases, drag coefficient decreases until Reynolds number reaches the range from 10^3 to 10^5, drag coefficient stay constant at 0.4 (for smooth sphere) which is the moderate Reynolds number.

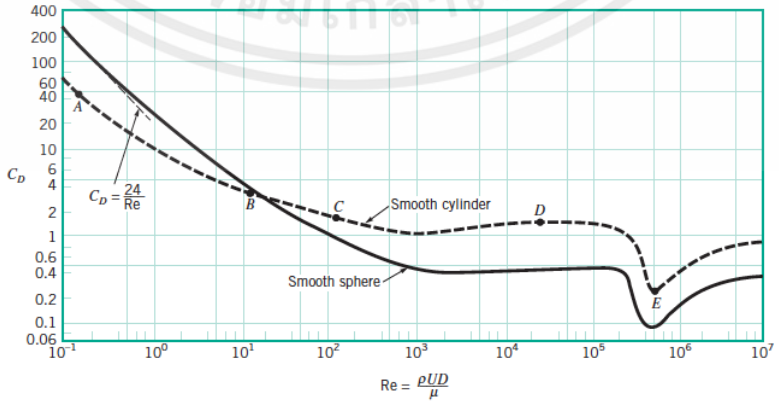

Figure 3.6 Moderate Reynold number drag coefficient

(https://www.chegg.com)

Reynolds number passes 10^5 is the range of large Reynolds number. For the blunt body object, the turbulent layer cause C_D to decreases during this range as shown in the figure below:

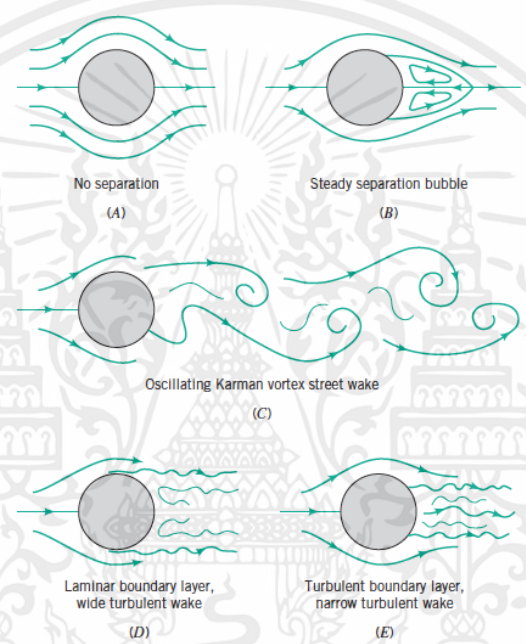

Figure 3.7 Turbulent flow

(https://www.chegg.com)

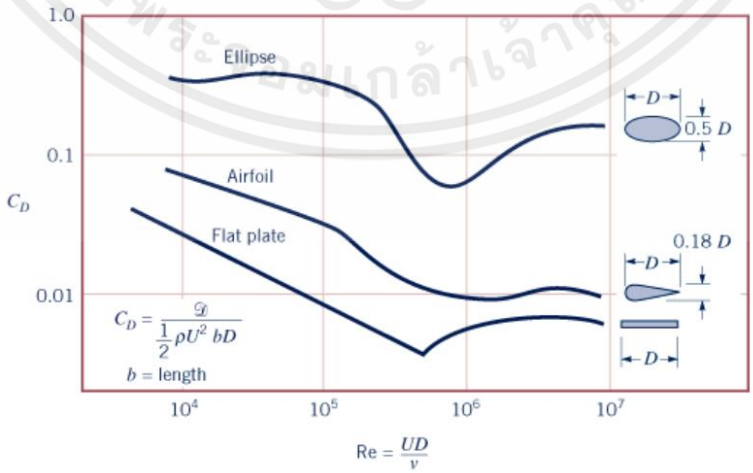

Figure 3.8 Character of the drag coefficient as a function of Reynolds number for object with various degree of streamlining, (two-dimensional flow)

(https://www.chegg.com)

3.2.2 Downforce

Downforce is created by wing or airfoil. Wing can be used for different application depend on its shape. To generate downforce for a racing car, the wing needs to be concave down so the pressure above the wing is greater than underneath it.

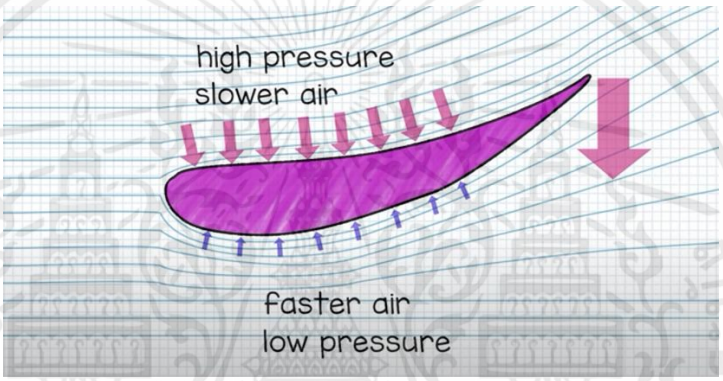

Figure 3.9 Downforce

(https://www.youtube.com)

According to the laws of aerodynamics, Downforce is the opposite of lift force and is caused by dividing the air. This causes the pressure under the abdomen to be lower than the upper surface. It creates pressure on the vehicle and helps it turn firmly. It can be calculated using the equation below.

$$C_L = \frac{L}{\frac{1}{2}\rho V^2 A}$$

L stands for lift per unit of width. The formula indicates how a symmetric airfoil's lift changes as the angle of attack α.

$$C_L = 2\pi\alpha$$

Since is measured in radians and C_L is a nondimensional number, the value in degrees must be multiplied by $\pi/180$. The effective angle of attack by α_{l0} for a cambered airfoil, but the coefficient 2π does not change. Thus, the symmetric airfoil will have zero lift at α = 0 while the cambered airfoil will have a lift of $c_l = 2\pi\alpha_{l0}$, even at zero angle of attack.

$$C_L = 2\pi(\alpha + \alpha_{L0})$$

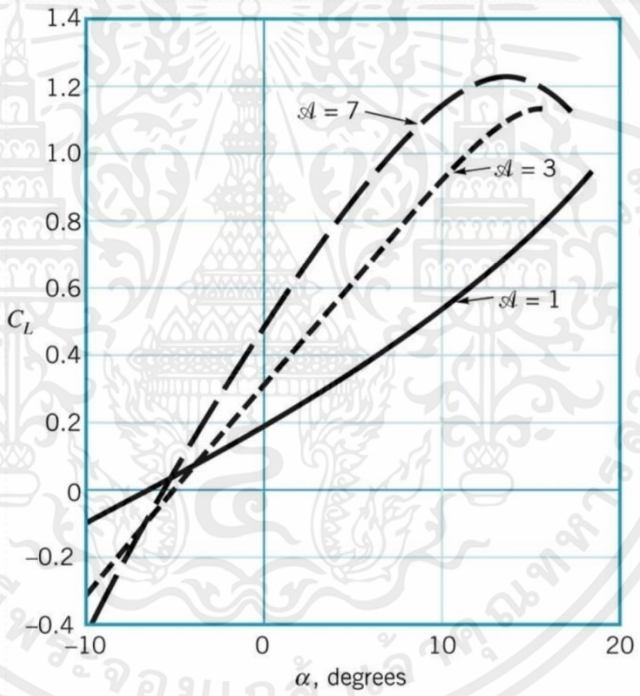

Figure 3.10 Typical lift coefficient data as a function of angle of attack and the aspect ratio of the airfoil.

(https://www.chegg.com)

3.3 Computational fluid dynamic

3.3.1 Computational fluid dynamic (CFD)

Computational fluid dynamic is the process of mathematic predicting physical fluid flow by solving the equations using computational power.

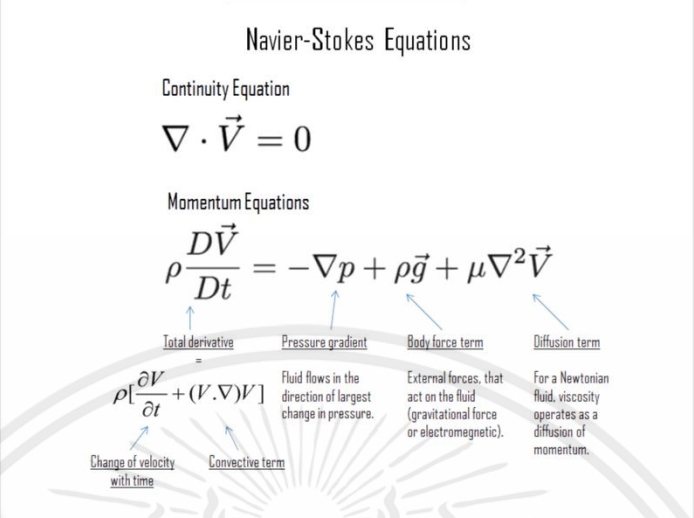

Figure 3.11 Navier-Stork equation

([https://www.thermal-engineering.org/what-is-navier-stokes-equation-definition/)

The most common (CFD) tools are based on the Navier-Stokes(N-S) equations. While the bulk of the terms in the Navier-Stokes equations remains constant, more terms can be added or removed based on the physics.

Navier-Stokes Equation

Conservation of Momentum which can be referred to as the Navier-Stokes.

$$\overbrace{\frac{\partial}{\partial t}(\rho\vec{v})}^{I} + \overbrace{\nabla\cdot(\rho\vec{v}\vec{v})}^{II} = \overbrace{-\nabla p}^{III} + \overbrace{\nabla\cdot\left(\overline{\overline{\tau}}\right)}^{IV} + \overbrace{\rho\vec{g}}^{V}$$

I: Local change with time

II: Momentum convection

III: Surface force

IV: Diffusion term

V: Mass force

The main structure of thermo-fluids examination is directed by governing equations that are based on the conservation law of fluid's physical properties.

The basic equations are the three laws of conservation.

1. Conservation of Mass: Continuity Equation
2. Conservation of Momentum: Newton' Second Law
3. Conservation of Energy: First Law of Thermodynamic or Energy Equation

These principles state that mass, momentum, and energy are stable constants within a closed system. In short, everything must be conserved.

In a CED software analysis, fluid flow and its associated physical properties, such as velocity, pressure, viscosity, density, and temperature, are calculated based on defined operating conditions. To arrive at an accurate, physical solution, these quantities are calculated simultaneously.

Computational fluid dynamics (CFD) has three primary stages, which are as follows:

Pre-processing begins with

1. The creation of geometry and meshing.
2. Simulation: Solving governing equations with a mesh model.
3. Post-processing and result analysis: it's critical to evaluate both the qualitative and quantitative aspects of projected physical attributes.

3.3.2 Computational mesh theory

When performing a CFD simulation, the equations of fluid mechanics are first solved in a solution domain, which designates a region of space with a particular geometric shape. For example, when modeling flow along a pipe, the solution domain would be an area of space where the fluid is located inside the pipe.

In meshing, the solution domain is divided into a mesh of tiny volumes or cells. The cells are made using computer programs and certain user specifications. We don't discuss the processes used by the meshing software or the software itself. Instead, in this chapter we define the structure and characteristics of a valid mesh.

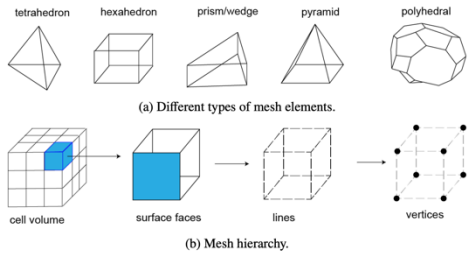

Figure 3.12 (a) Types of mesh elements including tetrahedron, hexahedron, prism/wedge, pyramid, and polyhedral. (b) Mesh topology demonstrating the hierarchy for each level of meshing.
(https://www.mr-cfd.com/y-and-grid-types/)

3.3.3 Turbulence equation

The formals as show below are stand for classify a turbulent flow. This formal is K-Epsilon model. K-Epsilon is use two equations for adjust value of K: Turbulence kinetic energy (4) and e: rate of dissipation (5) to define air flow pattern. In this formal is subset of K-epsilon, A functional K-epsilon was used that changes the turbulent viscosity formula A new transport equation for The decay rate $\in$ was obtained from the exact equation for the transport of Mean squared volatility, vorticity, and transport equation.

$$\frac{\partial}{\partial t}(\rho k) + \frac{\partial}{\partial x_j}(\rho k u_j) = \frac{\partial}{\partial x_j}\left[\left(\mu + \frac{\mu_t}{\sigma_k}\right)\frac{\partial k}{\partial x_j}\right] + G_k + G_b - \rho\epsilon - Y_M + S_k \qquad (4)$$

$$\frac{\partial}{\partial t}(\rho\epsilon) + \frac{\partial}{\partial x_j}(\rho\epsilon u_j) = \frac{\partial}{\partial x_j}\left[\left(\mu + \frac{\mu_t}{\sigma_\epsilon}\right)\frac{\partial \epsilon}{\partial x_j}\right] + \rho C_1 S_\epsilon + \rho C_2 \frac{\epsilon^2}{k+\sqrt{v\epsilon}} + C_{1\epsilon}\frac{\epsilon}{k}C_{3\epsilon}G_b + S_\epsilon \qquad (5)$$

3.3.4 Simulation algorithm theory

The simple algorithm of Patankar and Spalding (1972) states that the pressure-velocity coherence can be solved using an iterative solution.
In SIMPLE Algorithm:

- The convective fluxes through the cell surfaces are calculated from the predictable velocity components.
- A predictable pressure field is used to solve the momentum equations.
- A pressure correction equation is derived from the continuity & momentum equation.

- That Pressure Correction equation is solved to obtain a pressure correction field, which is in turn used to update the velocity and pressure fields that will satisfy the continuity equation.
- Again, Momentum equation is solved with the updated pressure and velocity field.
- The process is iterated until convergence of the velocity and pressure fields.

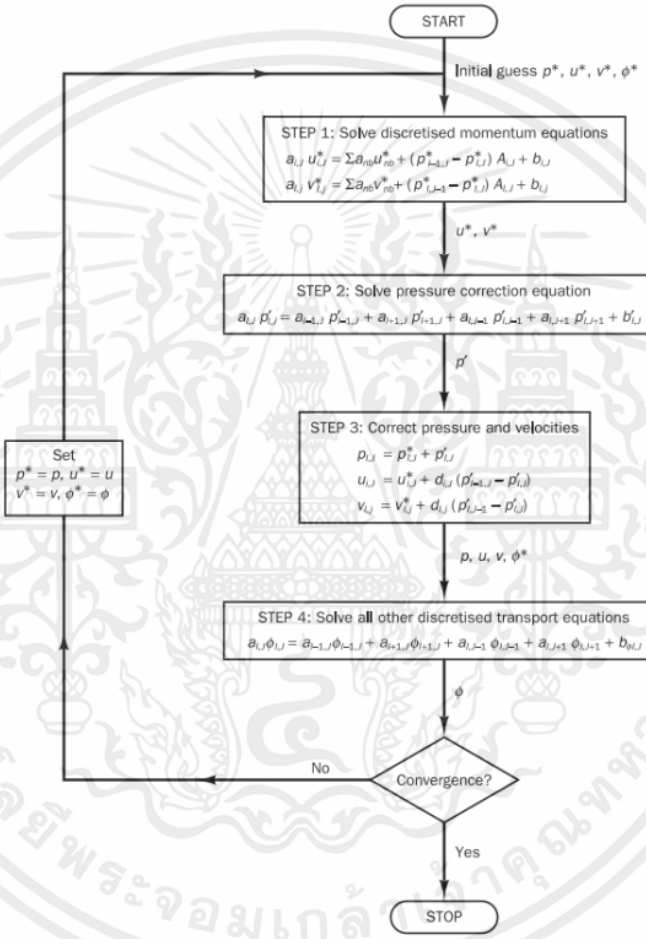

Figure 3.13 Flow chart of SIMPLE Algorithm
(https://commons.wikimedia.org/wiki/File:Flow_chart_for_SIMPLE_Algorithm.jpg)

The flow chart provides step-by-step instructions for how the SIMPLE algorithm works in Ansys Fluent. The process guessing the initial pressure field, deriving pressure correction, use the pressure correction to correct the pressure and velocity fields,

solving the momentum equation, and repeating the process until convergence is achieved.

Chapter 4

Methodology

4.1 Airfoil selection by using CFD

4.1.1 Airfoil preparation for simulation

Airfoil S1223, E423, and E421 are chosen to simulate lift coefficient due to various angle of attack. The airfoil coordinates are downloaded as script.

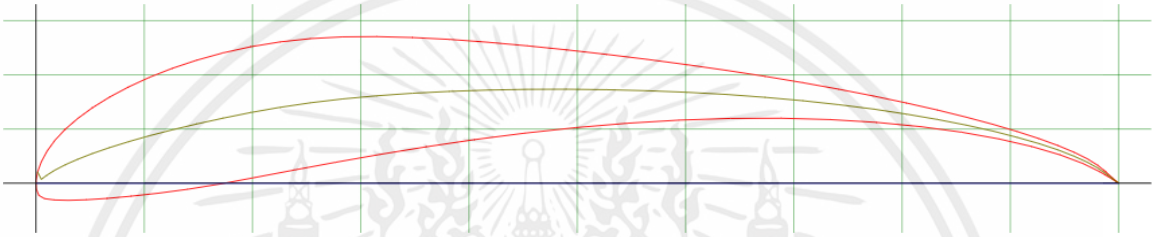

Figure 4.1 S1223 airfoil
(http://airfoiltools.com/)

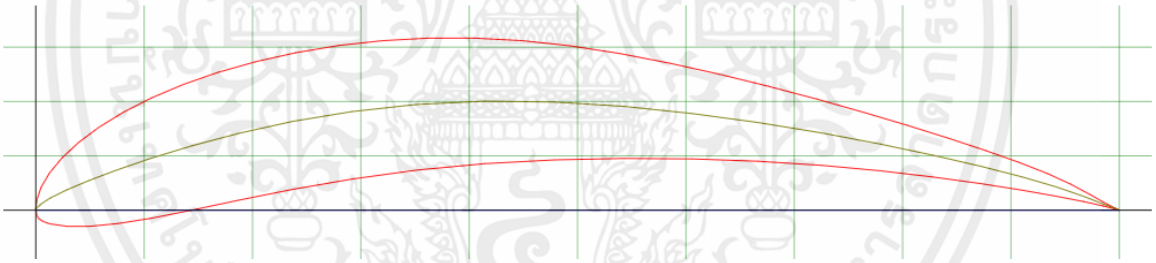

Figure 4.2 E423 airfoil
(http://airfoiltools.com/)

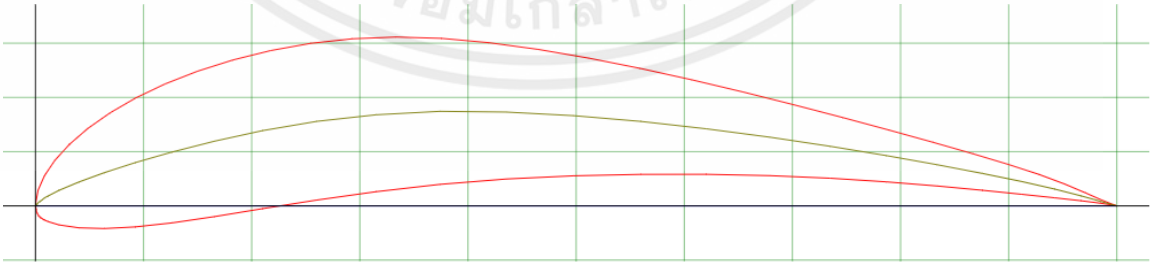

Figure 4.3 E421 airfoil
(http://airfoiltools.com/)

All airfoils are created in 3D in AutoCAD with the same chord and span which are 200mm and 1300mm, then all are exported as IGS file to prepare for CFD simulation.

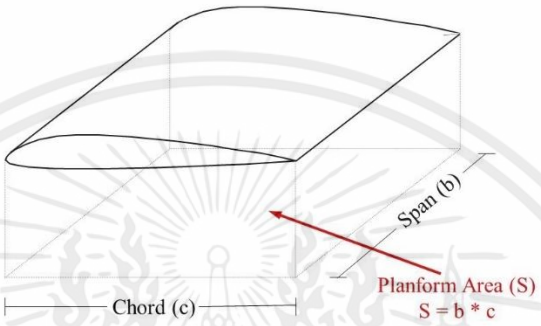

Figure 4.4 Airfoil geometry

(https://slideplayer.com/slide/5280118/)

4.1.2 Creating geometry for meshing

In Ansys (Workbench), import IGS file of an airfoil into fluent geometry.

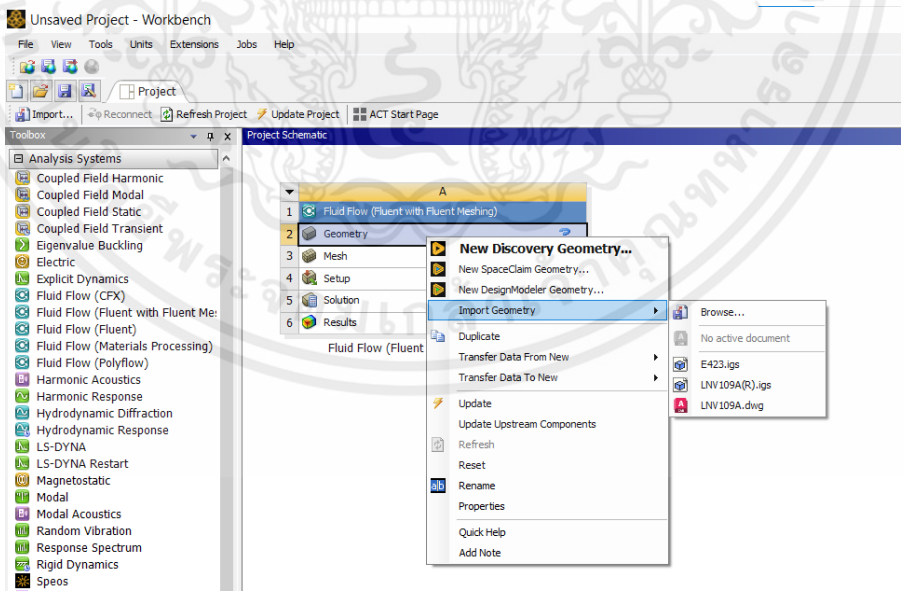

Figure 4.5 Airfoil Import

Create geometry fluid boundary in Design Modeler using cube with the length (parallel to chord) of 1200mm and height (perpendicular to chord) 1000mm and width (equal to span) 1300mm. Changing part to fluid domain by subtracting the airfoil from the boundary. Fluid domain is the area where air can flow and the part that is subtracted out will act as a wall to guide the flow.

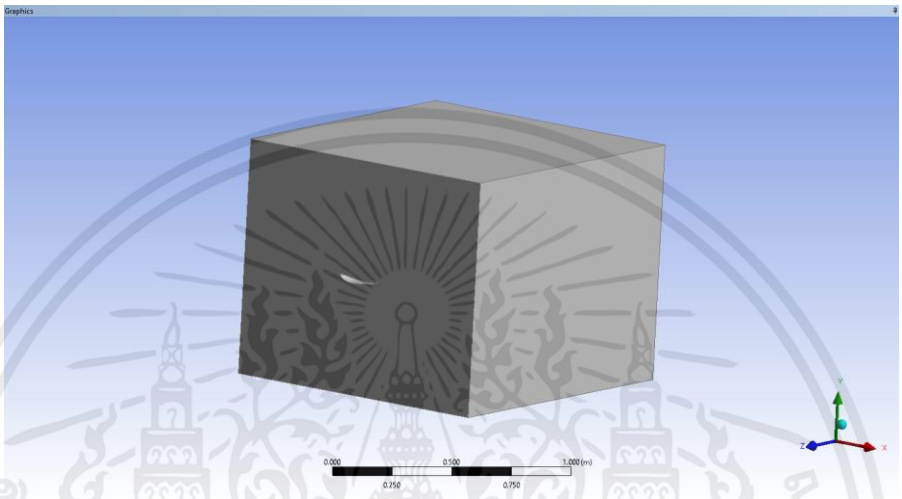

Figure 4.6 Airfoil boundary

Mesh using fluent meshing. To get good simulation and reliable results, good quality meshing is required. Sizing is the way to get good quality mesh. A smaller size mesh is a better mesh quality, but the time used to mesh and simulate will be longer. Another method to better the mesh quality is to add boundary layer to the model and apply smooth transition on the wall to get a precision mesh. The last feature to achieve 0.25 cell quality is to improve mesh quality on both surface and volume.

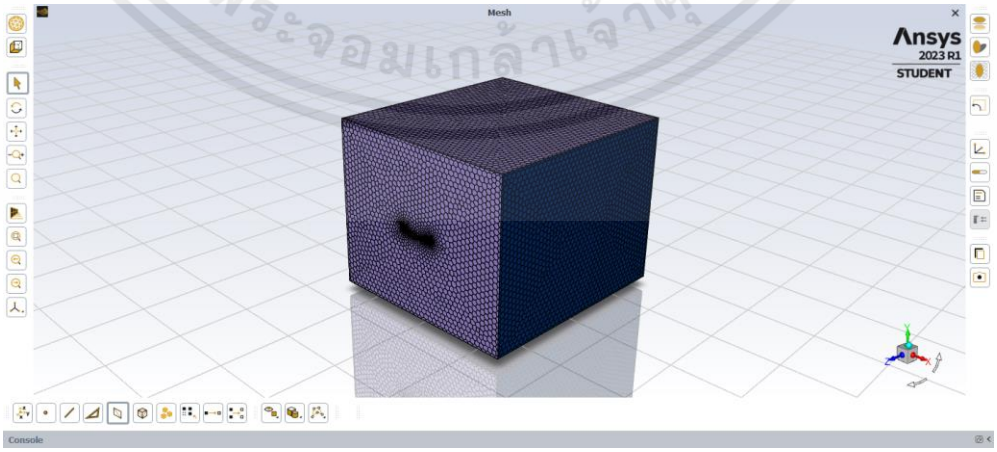

Figure 4.7 Airfoil boundary meshing

The number of cells is provided to show the quality of the mesh. More cells mean better quality but comes with more time consuming when simulation. The only problem is the version of Ansys used for this project is a student version and it limits the number of cells to approximately 500,000 cells.

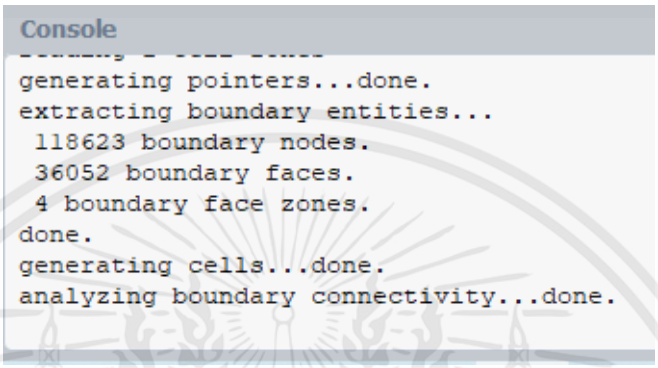

Figure 4.8 Number of cells

The number of cells and the quality of the mesh is important. Bad quality mesh will result in an error in simulation process, or the residual number would converge and that makes the result data unreliable.

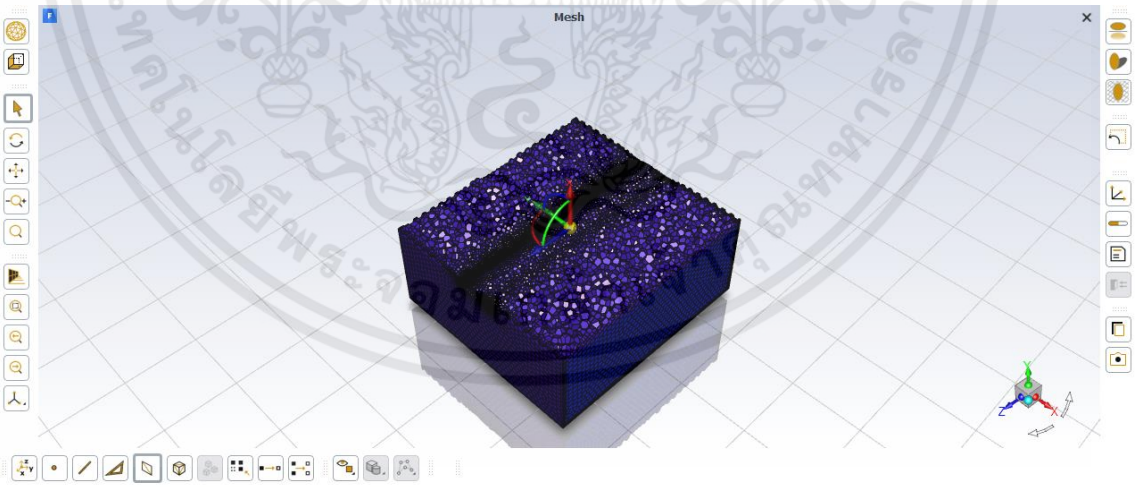

Figure 4.9 0.21 mesh quality

4.1.3 Airfoil simulation

For simulation condition use K-omega and set as turbulence model. The scheme of simulation is Coupled. For spatial discretization, Pressure and Momentum are second order, Turbulence Kinetic Energy and Specific Dissipation Rate are first order.

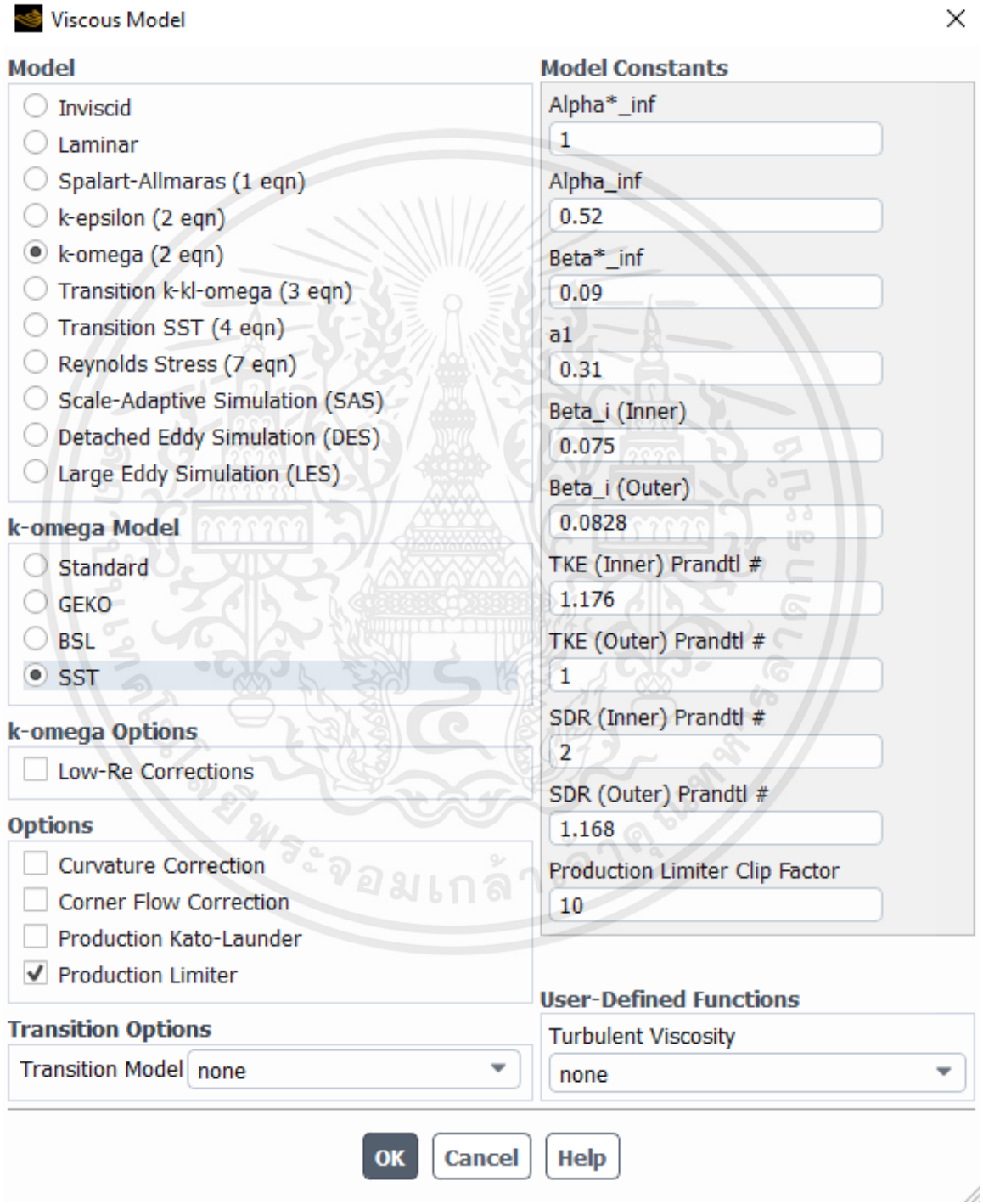

Figure 4.10 Model condition

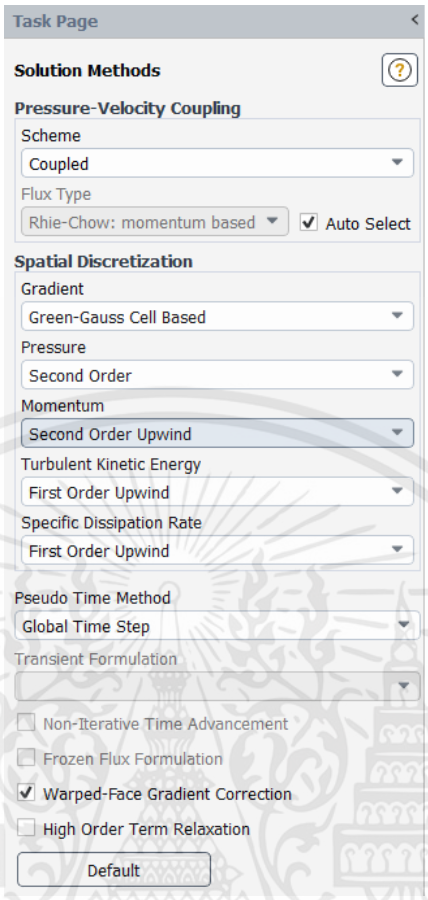

Figure 4.11 Scheme of simulation

The inlet airflow is set to 16.8 m/s as the formula student car runs with the average speed of 60 km/h. All scale residual is set to below 1×10^{-5} for proving convergence. The simulation takes around 200 iterations to converge with the condition.

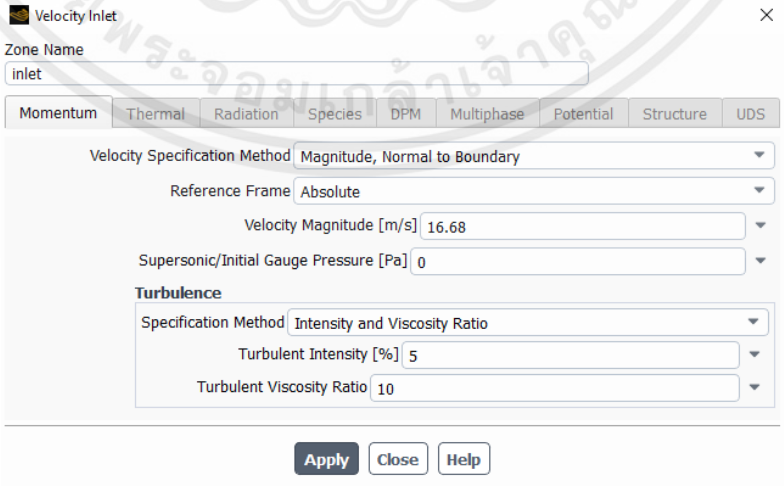

Figure 4.12 Inlet velocity

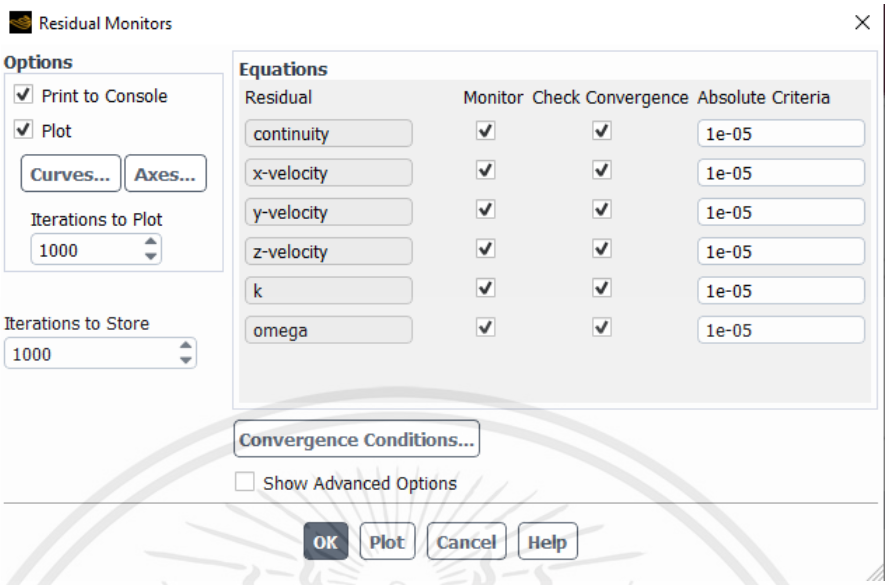

Figure 4.13 Scale residual

After all the data is computed, initialize with hybrid solution then run the simulation. All the process is the same when simulating each airfoil. Collect the results of lift force and drag force of 3 airfoils and use the data to calculate for lift coefficient and drag coefficient.

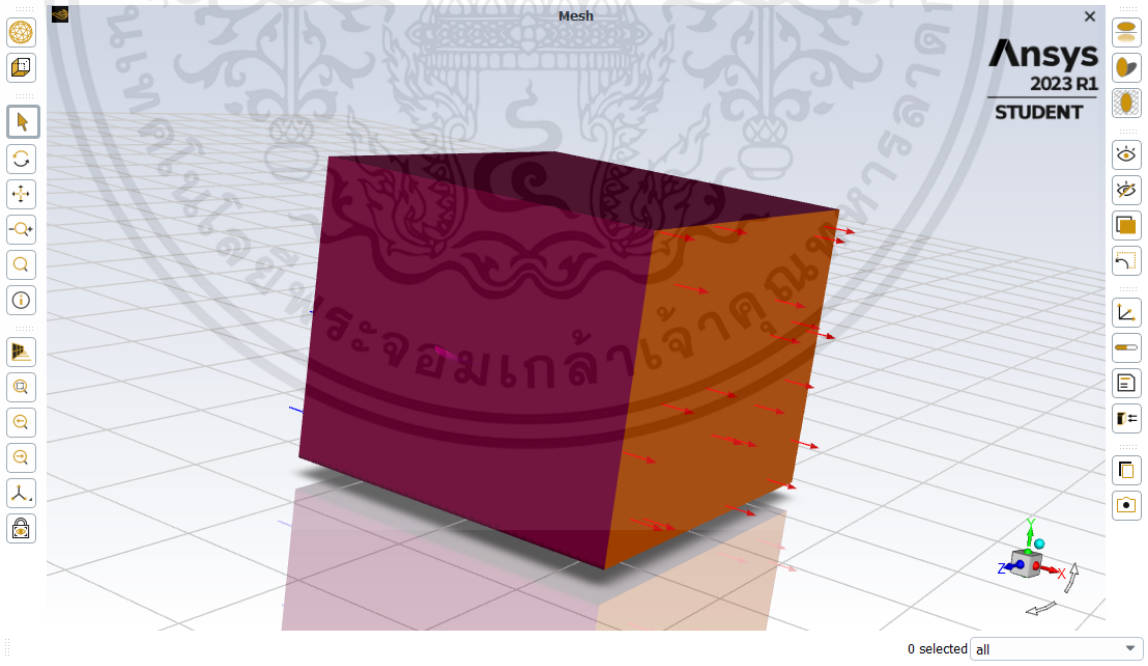

Figure 4.14 Run simulation

The formula uses to calculate for lift and drag coefficient are:

$$C_L = \frac{L}{\frac{1}{2}\rho V^2 A}$$

$$C_{Dp} = \frac{D_p}{\frac{1}{2}\rho \vartheta^2 A}$$

Compute for C_L and C_D of each airfoil using lift and drag force.

Table 4.1 S1223 Simulation Data

S1223 AoA	Drag Force (N)	Drag Project Area(X)	Cd	Downforce (N)	Lift Project Area(Y)	Cl
-5	3.6273743	0.04674845	0.456059487	12.414308	0.2599999	0.28063748
-4	2.9470522	0.04500855	0.384847921	19.115893	0.2599999	0.43213331
-3	2.3286266	0.0433921	0.31541731	27.919221	0.2599999	0.63114109
-2	1.843115	0.0418762	0.258691111	35.431812	0.2599999	0.8009705
-1	1.5361188	0.04049703	0.222945119	44.355051	0.2599999	1.00268898
0	1.6001679	0.03917299	0.240090608	48.699293	0.2599999	1.10089478
1	1.6896337	0.03822026	0.259833572	52.783817	0.2599999	1.19322941
2	1.781748	0.04142381	0.252809027	58.868076	0.2599999	1.33076999
3	1.8917986	0.04469442	0.248781414	63.682673	0.2599999	1.43960863
4	2.0284863	0.04798019	0.248488591	67.200979	0.2599999	1.51914335
5	2.2174413	0.05132354	0.253940439	74.123933	0.2599999	1.67564345
6	2.3771546	0.05468004	0.255520025	77.777875	0.2599999	1.75824435
7	2.5261377	0.058047	0.25578412	79.797275	0.2599999	1.80389485
8	2.752746	0.06145927	0.263254062	85.453638	0.2599999	1.93176242
9	3.0318112	0.06490299	0.2745578	89.585631	0.2599999	2.02517014
10	3.2226856	0.06835172	0.277118059	93.486816	0.2599999	2.11336021
11	3.5098459	0.07181691	0.287248436	96.835418	0.2599999	2.18905861
12	3.9549675	0.07527857	0.30879332	100.02101	0.2599999	2.26107201
13	4.5251685	0.07877876	0.33761517	101.53683	0.2599999	2.29533859

14	6.6248259	0.08230197	0.473108311	93.545859	0.2599999	2.11469493
15	8.7482161	0.08584324	0.598976439	85.244735	0.2599999	1.92703997
16	9.9349717	0.08935225	0.653517888	80.738257	0.2599999	1.82516666
17	11.526735	0.09290524	0.729226492	72.369503	0.2599999	1.63598285
18	13.141364	0.09646632	0.800683856	70.923002	0.2599999	1.60328329
19	14.848489	0.1000339	0.872431623	69.913083	0.2599999	1.58045309
20	16.070876	0.1035693	0.912021019	66.184962	0.2599999	1.4961753
21	17.3327	0.1071569	0.950697643	65.608177	0.2599999	1.48313652
22	18.966291	0.1107196	1.006825577	63.475226	0.2599999	1.43491909
23	20.472275	0.114295	1.052774151	62.831005	0.2599999	1.42035585
24	21.789713	0.1178643	1.086589658	61.841248	0.2599999	1.39798143
25	24.070138	0.1214346	1.165017561	62.492046	0.2599999	1.41269335
26	24.9438	0.1249553	1.173287037	61.627913	0.2599999	1.39315879
27	27.220263	0.1284792	1.245247939	62.844463	0.2599999	1.42066008
28	28.652124	0.1320317	1.275483794	63.182151	0.2599999	1.42829384
29	30.356597	0.1355381	1.316400474	63.926316	0.2599999	1.44511642
30	31.727115	0.1390508	1.34107612	64.2039	0.2599999	1.45139147
31	32.77868	0.1424901	1.352082238	63.632668	0.2599999	1.43847822
32	34.48928	0.1459748	1.388681268	64.247161	0.2599999	1.45236943
33	36.704667	0.1493905	1.444091281	65.506842	0.2599999	1.48084574
34	38.149595	0.1528077	1.467374714	65.31217	0.2599999	1.47644499
35	40.551825	0.1561678	1.526213357	66.251719	0.2599999	1.49768441
36	41.945199	0.1595167	1.545512211	65.851026	0.2599999	1.48862635
37	43.282742	0.1628289	1.562354617	65.331337	0.2599999	1.47687828
38	46.154624	0.1661099	1.633112259	66.875972	0.2599999	1.51179625
39	47.594211	0.1693567	1.651764345	66.212457	0.2599999	1.49679685
40	48.831555	0.1725899	1.662958899	66.212457	0.2599999	1.49679685

Table 4.2 E423 Simulation Data

E423 AoA	Drag Force (N)	Drag Project Area(X)	Cd	Downforce (N)	Lift Project Area(Y)	Cl
-5	3.4990747	0.05344353	0.3848171	11.70502	0.2599917	0.2646117
-4	2.7930944	0.05157516	0.3183035	18.709366	0.2599917	0.4229567
-3	2.2009834	0.04980819	0.2597242	25.861106	0.2599917	0.5846338
-2	1.767292	0.04811171	0.2159006	32.828294	0.2599917	0.7421389
-1	1.4323452	0.04649116	0.1810813	39.517247	0.2599917	0.8933539
0	1.4704882	0.04489371	0.1925185	44.191748	0.2599917	0.9990289
1	1.5487047	0.04380124	0.2078158	49.598919	0.2599917	1.1212671
2	1.6363943	0.0466846	0.2060206	54.459331	0.2599917	1.2311449
3	1.7468011	0.04959763	0.2070041	58.831571	0.2599917	1.3299867
4	1.8756161	0.05259743	0.2095925	63.501848	0.2599917	1.4355662
5	2.0275021	0.05564594	0.214153	67.773177	0.2599917	1.5321268
6	2.1934889	0.05868276	0.2196955	72.888701	0.2599917	1.6477718
7	2.3799203	0.06178914	0.2263845	77.691945	0.2599917	1.7563572
8	2.572587	0.06492458	0.2328934	82.104884	0.2599917	1.8561191
9	2.7585117	0.06813599	0.2379549	86.184472	0.2599917	1.9483451
10	3.0014085	0.0713634	0.2471985	90.623544	0.2599917	2.0486978
11	3.2583056	0.07460825	0.2566855	94.822876	0.2599917	2.1436307
12	3.5558952	0.07787327	0.2683842	99.04171	0.2599917	2.2390046
13	3.8883394	0.08118002	0.2815214	102.58316	0.2599917	2.319065
14	4.7317147	0.08454964	0.3289297	101.90395	0.2599917	2.3037103
15	5.0545134	0.08790593	0.3379539	105.87479	0.2599917	2.3934779
16	6.484237	0.09129394	0.4174585	100.38483	0.2599917	2.2693681
17	8.2877916	0.09472512	0.5142449	97.894148	0.2599917	2.213062
18	11.313478	0.09814598	0.6775166	82.209066	0.2599917	1.8584743
19	12.323258	0.1016195	0.7127625	79.501248	0.2599917	1.7972596
20	14.413731	0.1050515	0.8064371	72.852674	0.2599917	1.6469573
21	16.191089	0.1085281	0.8768599	69.438032	0.2599917	1.5697636
22	18.028014	0.1120029	0.9460519	65.265675	0.2599917	1.4754405
23	19.074999	0.1154833	0.9708266	64.315248	0.2599917	1.4539545
24	20.71033	0.1189631	1.0232249	61.745095	0.2599917	1.3958518

25	22.455622	0.1224783	1.0776116	60.913117	0.2599917	1.3770436
26	23.738396	0.1259302	1.107944	59.975519	0.2599917	1.3558476
27	24.846115	0.1294292	1.1282947	59.790958	0.2599917	1.3516753
28	26.044865	0.1328667	1.1521322	59.679756	0.2599917	1.3491614
29	27.798244	0.1363311	1.1984468	59.920074	0.2599917	1.3545941
30	29.367355	0.1397711	1.2349341	60.268138	0.2599917	1.3624627
31	30.901383	0.1432014	1.2683146	60.18356	0.2599917	1.3605507
32	32.583544	0.146603	1.3063267	60.832163	0.2599917	1.3752135
33	34.067352	0.1499698	1.3351526	61.061644	0.2599917	1.3804013
34	35.820938	0.1533354	1.3730643	61.500183	0.2599917	1.3903152
35	37.579559	0.1566975	1.4095677	61.695149	0.2599917	1.3947227
36	39.191673	0.1599931	1.439756	61.814474	0.2599917	1.3974203
37	41.11518	0.1632854	1.4799641	62.232381	0.2599917	1.4068677
38	42.752656	0.1665296	1.5089262	62.199693	0.2599917	1.4061288
39	44.436085	0.1697186	1.5388727	62.429259	0.2599917	1.4113185
40	46.124834	0.1729059	1.5679108	62.378947	0.2599917	1.4101811

Table 4.3 E421 Simulation Data

E421 AoA	Drag Force (N)	Drag Project Area(X)	Cd	Downforce (N)	Lift Project Area(Y)	Cl
-5	3.0297943	0.05265398	0.3382036	7.1919014	0.25993	0.1626236
-4	2.3690003	0.05112292	0.2723616	13.760606	0.25993	0.3111555
-3	1.7272846	0.04966425	0.2044167	20.618709	0.25993	0.4662313
-2	1.3397637	0.04823617	0.1632495	26.662443	0.25993	0.6028925
-1	1.351738	0.04689227	0.1694289	31.840902	0.25993	0.7199881
0	1.3890516	0.04559845	0.179046	37.009288	0.25993	0.8368559
1	1.4566361	0.04440336	0.1928109	42.337828	0.25993	0.9573451
2	1.5451225	0.04631232	0.1960933	47.438972	0.25993	1.0726924
3	1.6503823	0.04943784	0.1962101	52.033757	0.25993	1.1765899
4	1.7855377	0.05254962	0.1997081	57.142419	0.25993	1.2921072
5	1.9227664	0.0557165	0.2028332	61.727787	0.25993	1.3957918
6	2.0774634	0.05891832	0.2072428	66.529557	0.25993	1.5043696
7	2.2342609	0.06214783	0.2113023	70.746734	0.25993	1.5997287

8	2.4257294	0.06538197	0.2180624	75.489413	0.25993	1.7069704
9	2.6408585	0.06865086	0.2260974	80.43357	0.25993	1.8187679
10	2.8493619	0.07196254	0.232722	84.679593	0.25993	1.9147792
11	3.0816127	0.07528353	0.2405883	88.99707	0.25993	2.0124062
12	3.3296889	0.07861957	0.2489255	93.505621	0.25993	2.1143537
13	3.6359803	0.08195821	0.2607506	97.755243	0.25993	2.2104464
14	3.9419865	0.08534185	0.2714872	101.12883	0.25993	2.2867301
15	4.8379743	0.08874854	0.3204046	101.71478	0.25993	2.2999797
16	4.7366092	0.09217088	0.302044	108.5523	0.25993	2.45459
17	6.8443571	0.09558177	0.4208758	99.548787	0.25993	2.2510021
18	9.2342917	0.09899315	0.5482704	93.375865	0.25993	2.1114197
19	11.199548	0.1024531	0.6424979	84.871268	0.25993	1.9191133
20	13.163778	0.1059067	0.7305559	75.67453	0.25993	1.7111562
21	14.799324	0.1093591	0.7953958	73.746019	0.25993	1.6675486
22	16.294733	0.1128107	0.8489719	69.256515	0.25993	1.5660318
23	17.856039	0.1162688	0.9026477	68.171216	0.25993	1.5414909
24	18.965373	0.1197496	0.9308585	65.194285	0.25993	1.4741764
25	20.334324	0.1232178	0.9699573	62.701552	0.25993	1.4178106
26	22.112863	0.1266516	1.0261967	59.514935	0.25993	1.3457547
27	23.663887	0.1301145	1.0689484	57.883379	0.25993	1.3088618
28	24.999407	0.133571	1.1000537	56.572184	0.25993	1.279213
29	26.346266	0.1369721	1.1305331	57.179595	0.25993	1.2929478
30	27.633194	0.1404095	1.1567272	57.347169	0.25993	1.296737
31	29.215634	0.1437991	1.1941407	57.806592	0.25993	1.3071255
32	30.787942	0.147161	1.2296578	58.048296	0.25993	1.312591
33	32.503882	0.1505198	1.269223	58.488656	0.25993	1.3225484
34	34.150072	0.1538663	1.3045011	58.71344	0.25993	1.3276312
35	35.775908	0.1571533	1.3380228	58.952983	0.25993	1.3330478
36	37.544104	0.1604353	1.3754289	59.306173	0.25993	1.3410341
37	39.04644	0.1636944	1.4019869	59.405253	0.25993	1.3432745
38	40.777953	0.166903	1.4360105	59.545649	0.25993	1.3464492
39	42.614514	0.1701243	1.4722702	59.884527	0.25993	1.3541119
40	44.422002	0.1732684	1.5068676	60.09727	0.25993	1.3589225

The drag and lift coefficient of 3 airfoils is plotted on the graph to compare the performance of each airfoil on various angles of attack.

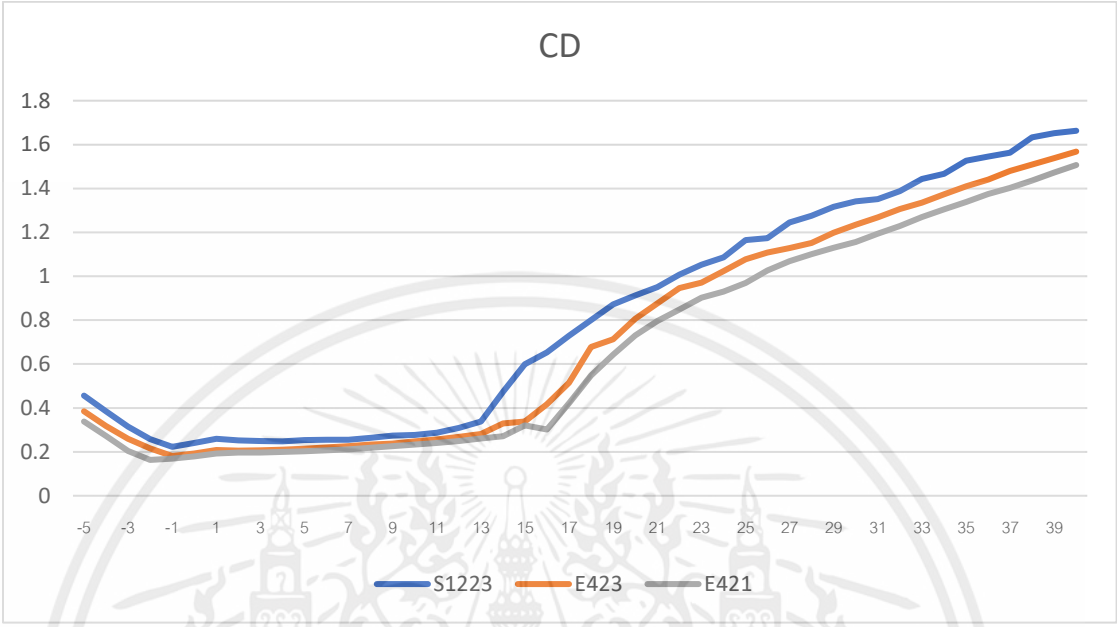

Figure 4.15 Cd comparison on 3 airfoils

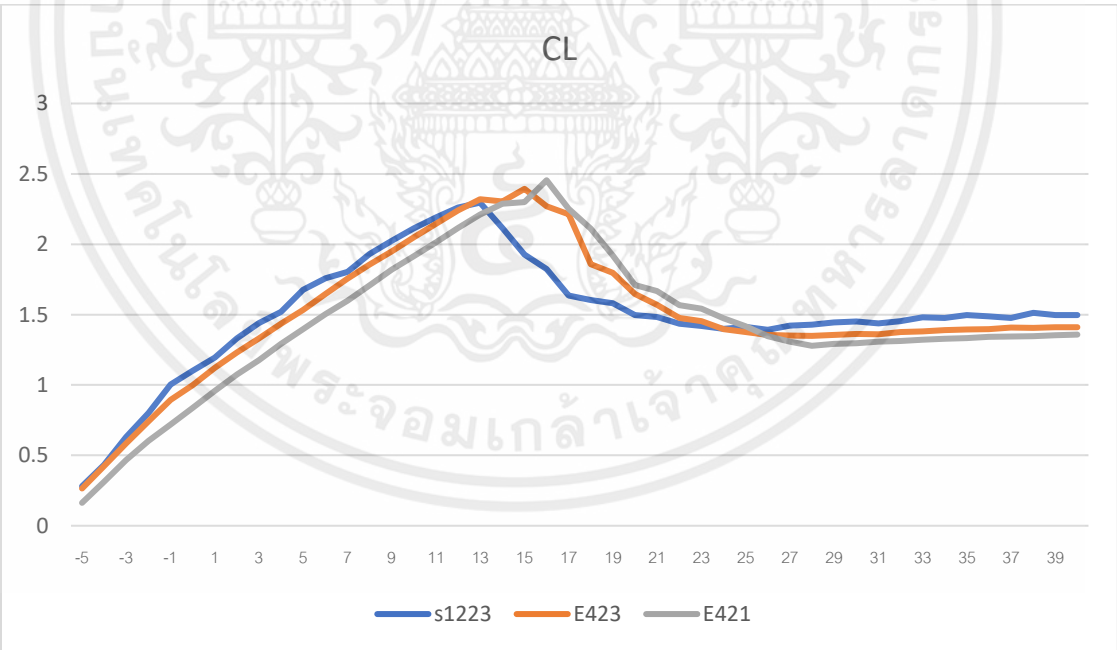

Figure 4.16 Cl comparison on 3 airfoils

After getting the result, the graphs above show that S1223 airfoil generates the best lift coefficient on the wider range of angles of attack and as in the reference

research, the angle of the 3rd flap could go up to above 40-degree, so we decide to use an S1223 airfoil on furthermore simulation of our front wing.

4.2 Draw 3D front wing

The front wing is consisting of 5 main elements:

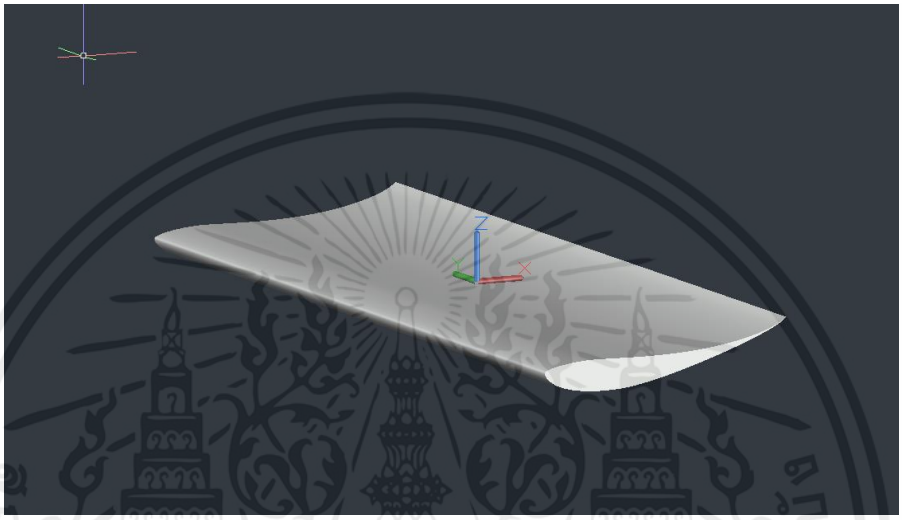

Figure 4.17 Main wing

Figure 4.18 Upper and lower flap

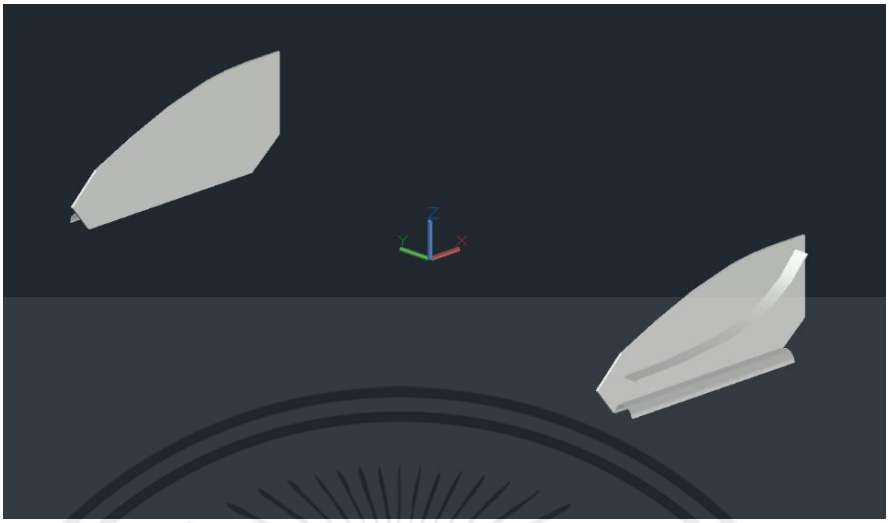

Figure 4.19 End plate

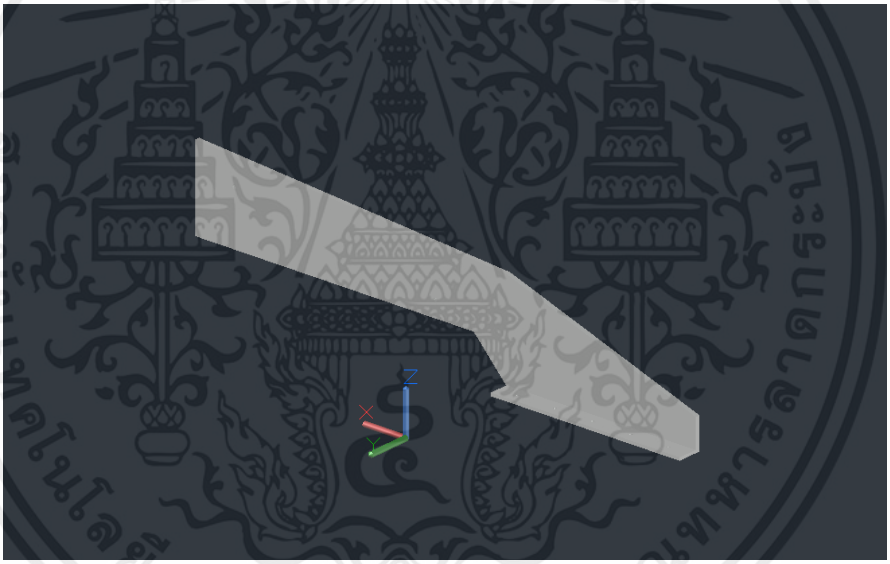

Figure 4.20 Central Vertical Plate

Put all the parts together to create a front wing. Set the main airfoil and both 2 flaps to 0-degree angle of attack and simulate for Cl and Cd so at the end, we can compare to the result and see how adjusting the wing to the right angle of attack is important and how it affects the car.

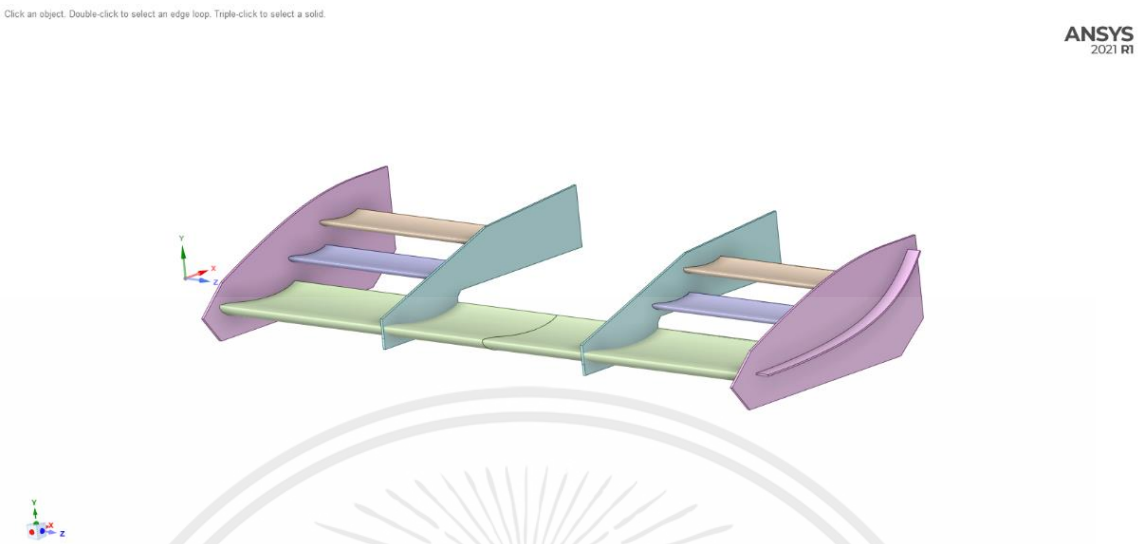

Figure 4.21 Front wing

Figure 4.22 0-degree front wing setup

The result from simulating 0°, 0°, 0° wing setting is Cd = 0.850592, Cl = 0.891277

4.3 Front wing simulation

4.3.1 Front wing preparation for simulation

Create front wing geometry boundary of the wing in design modeler, then do the meshing with high quality. Use all the method same as when simulating the airfoils. Slice the geometry in half to make it easier to run the simulation and reduce the time taking on running the simulation.

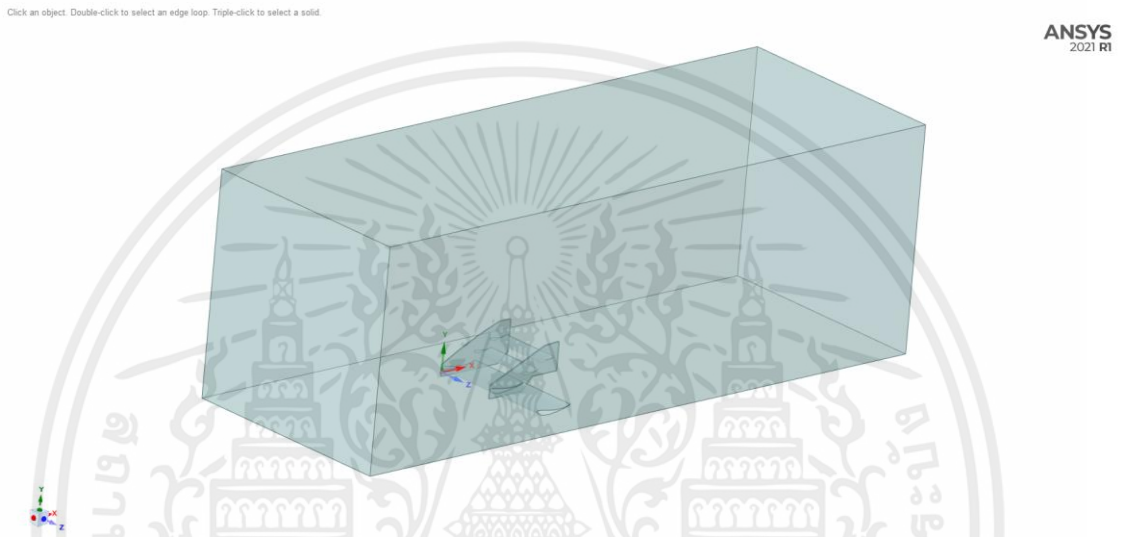

Figure 4.22 Front wing geometry boundary

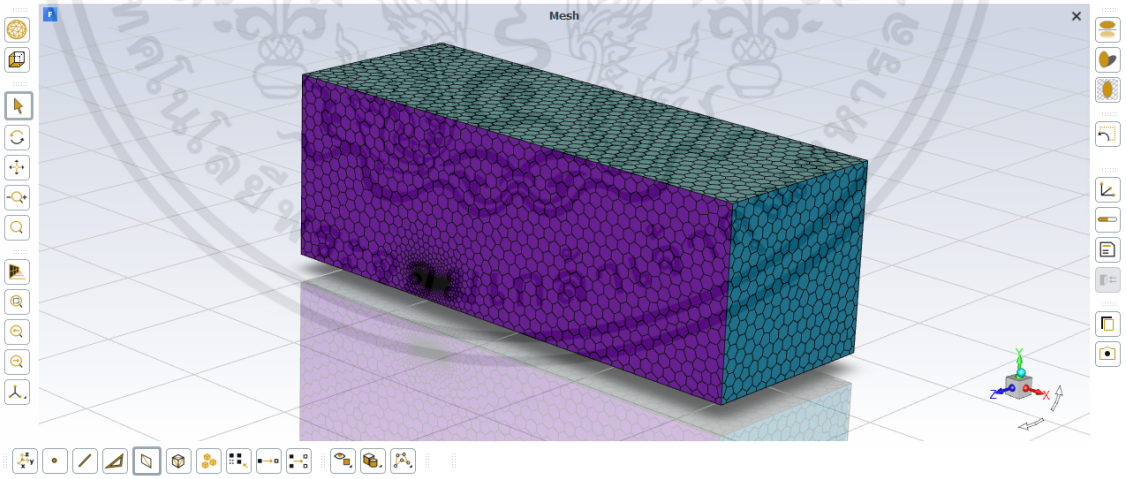

Figure 4.23 Front wing boundary meshing

Chapter 5

Result and discussion

5.1 Validation

5.1.1 Result Validation

From the result of airfoil simulation, we chose S1223 to develop our front wing. We will compare the experimental result to the standard values. From table 4.1 the maximum lift coefficient of S1223 is 2.295 at 13°. We compare this value to the standard value from airfoiltools website. First, we calculate for our airfoil Reynolds number, using the equation below:

$$Re = \frac{\rho v \ell}{\mu} = \frac{v \ell}{\mathcal{V}}$$

Where; ρ is 1.225 kg/m^3

v is 16.6667 m/s

ℓ is 0.2 m

$\mathcal{V}$ is 1.5111E-5 m^2/s

So the Reynolds number of our S1223 airfoil is 220,590.

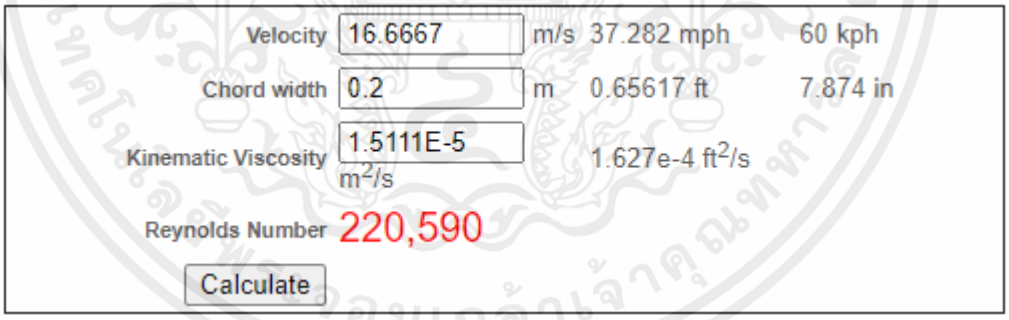

Figure 5.1 Reynolds number

(http://airfoiltools.com/)

Then we select 200,000 for the airfoil Reynolds number

Plot	Airfoil	Reynolds #
☐	s1223-il	50,000
☐	s1223-il	50,000
☐	s1223-il	100,000
☐	s1223-il	100,000
☐	s1223-il	200,000
☑	s1223-il	200,000
☐	s1223-il	500,000
☐	s1223-il	500,000
☐	s1223-il	1,000,000
☐	s1223-il	1,000,000

Figure 5.2 Reynolds number

(http://airfoiltools.com/)

```
     XFOIL         Version 6.96

Calculated polar for: S1223

1 1 Reynolds number fixed          Mach number fixed

xtrf =   1.000 (top)        1.000 (bottom)
Mach =   0.000     Re =     0.200 e 6     Ncrit =   5.000

  alpha    CL        CD       CDp       CM     Top_Xtr  Bot_Xtr
 ------ -------- --------- --------- -------- -------- --------

 13.000   2.2033   0.04609   0.03965  -0.1999   0.2439   1.0000
```

Figure 5.3 Standard Cl Cd value

(http://airfoiltools.com/)

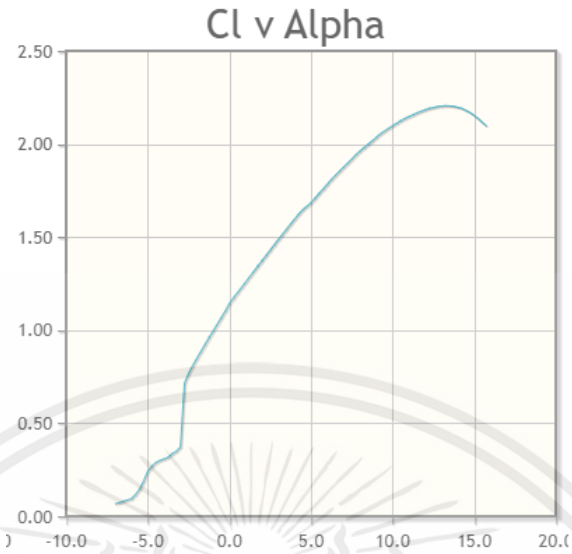

Figure 5.4 Standard Cl graph

(http://airfoiltools.com/)

According to the graph from airfoiltools website, maximum Cl value of S1223 is 2.2033 at 13° where our simulation value is 2.295, which is 4.16% error.

5.1.2 Simulation Validation

To choose a model for any kind of simulation, many factors are to be considered for the accurate and precise result. The basic things to consider are type of flow, accuracy requirement, and available computational resources. The simulation model we use in this thesis is k-omega (SST) which is the developed model that combines k-epsilon and k-omega together. K-epsilon is the model that is often used for external flow with complex geometry. It uses a wall function to analyze fluid flow close to the wall. On the other hand, standard k-omega model can be used without needing the distance from the wall. It shows good performance to the near wall geometry but it over predict separation. The SST model came from combining the advantage of those two models. It improves the prediction of the flow separation which the standard k-omega is not good at. When dealing with viscous sublayer and the turbulent boundary layer, this model is known to be the best of all others. The accurate flow separation prediction and turbulent boundary layer are crucial things when simulating flow over an airfoil.

That makes k-omega SST the most suitable model for an airfoil simulation, and it is the reason we use this model for the simulation.

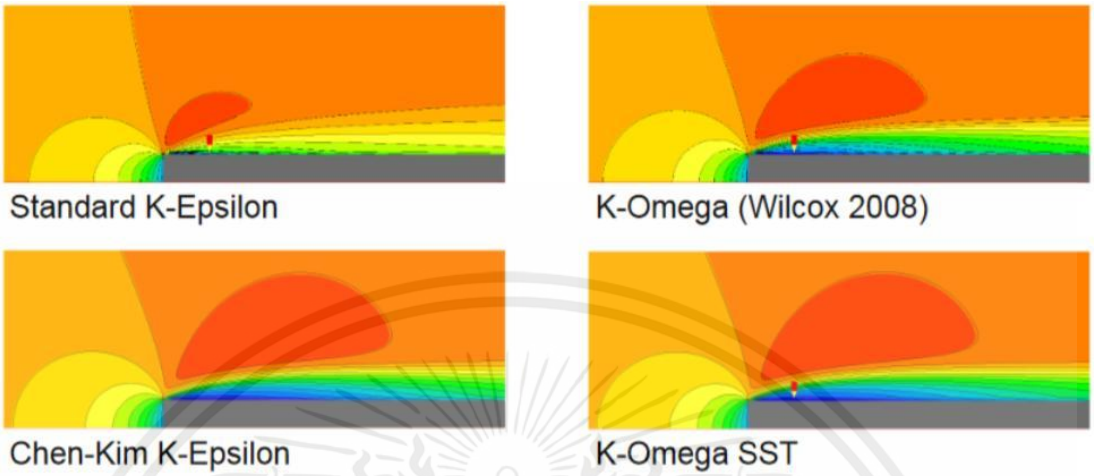

,

Figure 5.5 Simulation models comparison

(https://twitter.com/cham_uk/status/1143913192978026501?lang=zh-Hant)

5.2 Airfoil performance comparison

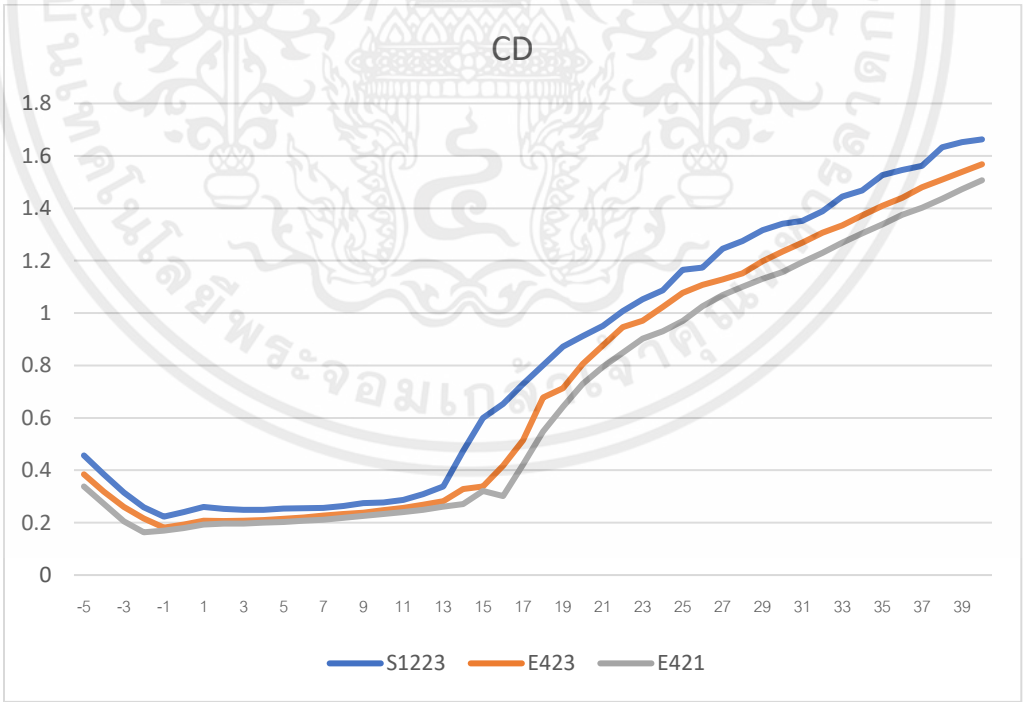

Figure 5.6 Drag coefficient on 3 airfoils

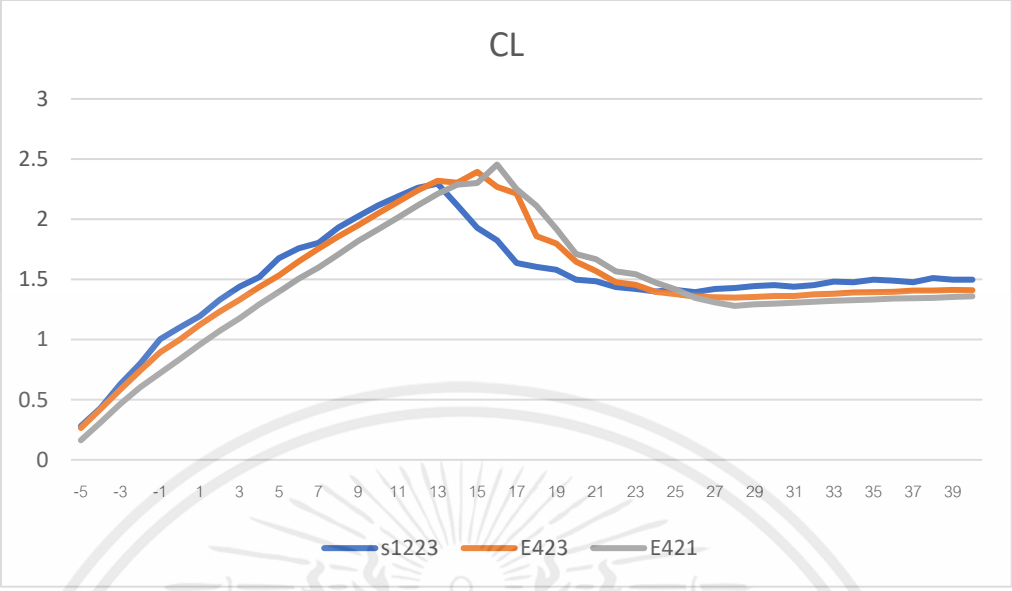

Figure 5.7 Lift coefficient on 3 airfoil

According to the drag coefficient graph, all 3 airfoils have almost the same coefficient value throughout the range of angles that have been chosen. They only differ about 0.1 so the other compiler we could analyze on deciding the best airfoil is the coefficient of lift. The graph shows that, from -5° to 13° S1223 generates the most lift coefficient, also from 26° to 40°, it gives the best performance. Although, E421 seems to show the best performance of all 3 at each peak but it only outperforms the other in a small range (15° to 25°) so we decide to use S1223 for all 3 elements of our front wing as each element would be set at different angle of attack, according to all research we have reviewed.

5.3 Angle of attack of 3 elements airfoil on front wing

Simulate the wing with various angles of attack on the main airfoil and flaps by using the same process as simulating the airfoils. On this 1st trial we set the angle of attack in the wide range to see which set of angles of attack gives most downforce with an acceptable drag force.

Table 5.1 First trial front wing simulation

AoA	Drag Force (N)	Drag Project Area(X)	Downforce (N)	Lift Project Area(Y)
0,0,0	4.564	0.03153703	29.04	0.1915051
1,10,20	8.0885	0.04279824	50.812	0.1895005

1,15,25	9.7991	0.04728111	56.145	0.1884506
1,20,30	11.599	0.05154745	60.79	0.1871763
1,25,35	13.277	0.05555599	64.14	0.1856901
1,30,40	14.215	0.05755863	64.63	0.182821

Table 5.2 First trial front wing simulation (continued)

AoA	Cd	Cl	Cl/Cd
0,0,0	0.85059178	0.891276808	1.04783144
1,10,20	1.11080651	1.575985682	1.41877605
1,15,25	1.21813344	1.751095774	1.43752377
1,20,30	1.32254269	1.908875586	1.44333759
1,25,35	1.4046412	2.030189343	1.44534373
1,30,40	1.45155252	2.077803216	1.43143509

The main airfoil is set to a low angle to create more adjustable room for the 2nd flap. The result from the first trial seems that 1°,10°,20° and 1°,15°,25° gives the best performance as the drag coefficient is not too high but all Cl/Cd are in the same range.

The 2nd trial data is chosen with respect to the 1st trial as listed below.

Table 5.3 Second trial front wing simulation

AoA	Drag Force (N)	Drag Project Area(X)	Downforce (N)	Lift Project Area(Y)
1,15,30	11.265	0.04939248	60.439	0.1871804
2,15,30	11.564578	0.05110564	62.459098	0.1871814
3,15,30	11.890262	0.05257421	64.506657	0.1870718
4,15,30	12.229187	0.05438006	66.359385	0.1870733
5,15,30	12.617404	0.05587544	68.54818	0.1869795

Table 5.4 Second trial front wing simulation (continued)

AoA	Cd	Cl	Cl/Cd
1,15,30	1.34049964	1.897812214	1.415749887
2,15,30	1.33001732	1.961233736	1.474592629

3,15,30	1.329275521	2.026714379	1.524675921
4,15,30	1.321764982	2.08490794	1.577366604
5,15,30	1.32722756	2.154756863	1.6235022

On this trial, the chosen angle result in some higher lift coefficient with some great Cl/Cd values but the drag coefficient still high. The angle of 5°,15°,30° gives the best value in this trial, it gives the lift coefficient of 2.154756863 and 1.6235022 for Cl/Cd but we still need to lower the drag coefficient. We aim to get the drag coefficient around 1.2 so some angles need to be adjusted for the better values. 5° degree for the main airfoil seems to give high lift coefficient so on the next trial we will keep the main airfoil to 5° degree and nearby value and adjust the other 2 flaps for lower drag coefficient.

The 3rd trial data is chosen with respect to the 2nd trial as listed below.

Table 5.5 Third trial front wing simulation

AoA	Drag Force (N)	Drag Project Area(X)	Downforce (N)	Lift Project Area(Y)
4,13,25	10.584	0.05137495	62.058	0.1883401
4,13,30	11.997	0.05344409	65.845	0.1870789
4,13,28	11.45	0.05260789	64.565	0.1876082
5,13,25	10.904	0.05286231	63.801	0.1882428
5,13,28	11.776	0.05412522	66.057	0.1875037

Table 5.6 Third trial front wing simulation (continued)

AoA	Cd	Cl	Cl/Cd
4,13,25	1.210862299	1.936650787	1.59939804
4,13,30	1.31937822	2.068684844	1.567924052
4,13,28	1.279236792	2.022747518	1.581214308
5,13,25	1.212372408	1.992073921	1.64312047
5,13,28	1.278775952	2.070643543	1.619238725

The set of 5°,13°,25° and 5°,13°,28° seems to be the result we are looking for, as the drag coefficient is close to 1.2 and lift coefficient is more than 2. The next trial, we will try to adjust some angle to see whether we can better the result.

The 4th trial data is chosen with respect to the 3rd trial as listed below.

Table 5.7 Forth trial front wing simulation

AoA	Drag Force (N)	Drag Project Area(X)	Downforce (N)	Lift Project Area(Y)
5,13,30	12.357	0.05497135	67.799	0.1869765
5,12,32	12.77	0.0554936	68.543	0.1864471
5,12,25	10.807	0.05243697	63.634	0.1882385
5,12,27	11.335477	0.05328395	64.952467	0.1877131
5,11,25	10.726708	0.05201427	63.37691	0.1882437

Table 5.8 Forth trial front wing simulation (continued)

AoA	Cd	Cl	Cl/Cd
5,13,30	1.321213438	2.131241187	1.613093786
5,12,32	1.352521994	2.160746481	1.597568461
5,12,25	1.211333983	1.986905026	1.640261938
5,12,27	1.2503734	2.033749257	1.626513533
5,11,25	1.212105129	1.978822996	1.632550633

The result we get on this trial is slightly different from the previous trial but as we try to keep the drag coefficient close to 1.2 along with the high drag coefficient, the most suitable and best value would be the set of 5°,13°,25°, as it generates 1.992073921 lift force (downforce) with the least drag coefficient of 1.212372408.

5.4 Front Wing Analyzation

The analyzation of each airfoil on the front wing is done by differing each one by 5 degree. We started with the main airfoil (lowest) by setting the 2nd and 3rd flap to 5 and 20 degrees, respectively, then set the main airfoil to 0 and 5 degrees. The result

shows that the coefficient of lift increases 0.32 along with 0.04 increases in drag coefficient.

Table 5.9 Main Wing Analyzation

AoA	Cl	Cd
0,5,20	1.434394	1.057941
5,5,20	1.758347	1.103103

For the 2nd flap, the main airfoil and the 3rd flap are frozen at 5 and 10 degrees, respectively. The 2nd flap is set to 5 and 10 degrees. The 5 degrees difference result in 0.05 increases in lift coefficient and 0.003 increases in drag coefficient.

Table 5.10 2nd Flap Analyzation

AoA	Cl	Cd
5,5,10	1.499299	0.949818
5,10,10	1.550832	0.952377

For the 3rd flap, both main airfoil and the 2nd flap are frozen at 5 degrees. The 3rd flap is set to 10 and 15 degrees. The result shows that the coefficient of lift increases 0.13 along with 0.06 increases in drag coefficient.

Table 5.11 3rd Flap Analyzation

AoA	Cl	Cd
5,5,10	1.499299	0.949818
5,5,15	1.630026	1.018706

From this experiment, the main airfoil and the 3rd flap have more effect on both lift and drag coefficient than the 2nd flap as the value increases in lift and drag coefficient of the 2nd flap are only 0.05 and 0.003. The airfoil that has most effect on the front wing is the main airfoil as the increases of the lift and drag coefficient are 0.32 and 0.04 but the 3rd flap only has 0.13 and 0.06 increases in lift and drag coefficient.

All the results can be sum up that the 2nd flap has less effect on Cl than the main airfoil 84.37% and Cd 92.5%. The 3rd flap has less effect on Cl than the main airfoil 59.37% and more effect on Cd than the main airfoil 50%. The main airfoil is the most effective, then the 3rd and 2nd, respectively; 1st > 3rd >2nd.

Chapter 6

Conclusion

6.1 Conclusion

1. Airfoil S1223 is chosen over E423 and E421 due to the performance it gives throughout the angle, Although, E423 and E421 have greater value of Cl at their peaks.

2. Drag coefficient of all 3 airfoils only differ by 0.1, so Cd values are not to be considered in the process of selecting the airfoil.

3. As we analyze the front wing, we know that the main airfoil has the most effect on the whole wing, so we try to increase the angle to the highest as possible but as we raise the angle to 6 degrees the simulation was error. We assume that it was stuck with the 2nd flap or some other element so the highest possible angle for the main airfoil is 5 degrees.

4. On the process of choosing angles for each airfoil on the front wing, we tried set all the angle in the wide range to see what the result gives us. As we proved that main airfoil has the most effect on the whole wing and the highest possible is 5 degrees due to the reasons, we gave earlier so we only deal with the 2nd and 3rd flap. Both flaps are adjusted according to the result of each trial until we get the best result.

5. In the final trial, the sets of angles that give the best performance are 5,13,25, 5,12,25, and 5,12,27 which all give most the same Cl and Cd, so we compare the Cl/Cd values of three of them. The first set has 1.643 and the 2nd and 3rd have 1.640 and 1.626, so the best of all set is 5,13,25 which gives 1.212 of Cd and 1.992 of Cl.

6. This simulation research considered only the front wing, not the whole car.

7. If we can do the simulation with the whole car, the rear wing and car body will be taken to account and we could also do the balancing between the front and rear wing for the perfect balance of downforce of the whole car, so that the front wing would not generates too much amount of downforce in front rather than the back or too least so that the front wing would not keep the front tires to the ground as the car goes through sharp corner in high speed, and the results would be more precise and accurate and could really be apply to the real car.

Reference

[1] Ben granger, Kyle Richards, Front wing design documentation, Illinois, 2016

[2] Wael A. Mokhtar, Jonathan Lane, Racecar Front Wing Aerodynamics, Lake Superior University, 2008

[3] Henrik Dahlberg, Aerodynamics development of Formula Student race car, KTH Mechanics, 2014

[4] https://engineeringexpo.uic.edu/news-stories/formula-sae-front-wing/

[5] https://www.racecar-engineering.com/articles/tech-explained-formula-student-aerodynamics/5/

[6]https://www.engineersedge.com/fluid_flow/aerodynamics_airfoil_theory_equations__15301.htm

[7] https://www.researchgate.net/

[8] https://www.sae.org/

[9] https://aip.scitation.org/doi/pdf/10.1063/1.5024107

[10] https://www.simscale.com/blog/formula-student-aerodynamics/

[11] https://www.simscale.com/docs/simwiki/cfd-computational-fluid-dynamics/what-is-cfd-computational-fluid-dynamics/

[12] https://juser.fz-juelich.de/record/885994/files/2020_Lintermann_ClinBiomedEng_Ch6.pdf

[13] https://web.stanford.edu/class/me469b/handouts/turbulence.pdf

[14] https://www.mr-cfd.com/services/fluent-modules/discrete-phase-model-dpm/

[15] http://airfoiltools.com/

[16] https://www.quora.com/

[17] https://www.diva-portal.org/smash/get/diva2:737287/fulltext01.pdf

[18] https://core.ac.uk/download/pdf/160501318.pdf

[19] https://iopscience.iop.org/article/10.1088/1742-6596/1635/1/012025/pdf

[20] https://www.nal.res.in/themes/stark/cfdimgs/FullPaper/P14-Design%20optimization%20%20of%20Front%20wing.pdf